

AD-A151 413

TRANSFORMATION TOUGHENED CERAMICS A POTENTIAL MATERIAL  
FOR LIGHT DIESEL E. (U) MICHIGAN UNIV ANN ARBOR DEPT OF  
MATERIALS AND METALLURGICAL E. T Y TIEN JUN 84

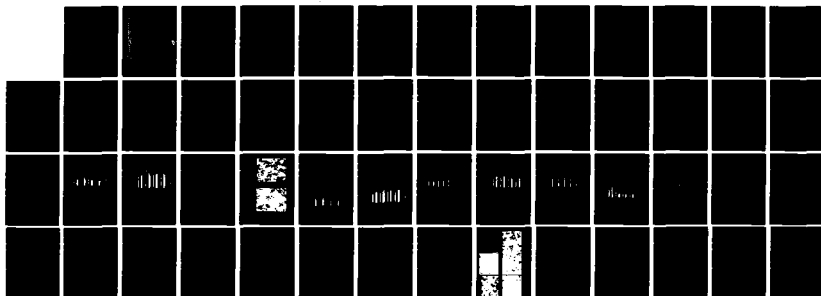
1/1

UNCLASSIFIED

AMRC-TR-84-26 DAAG46-82-C-0080

F/G 11/2

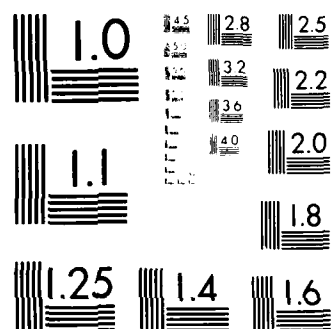
NL



END

FIMED

DEC

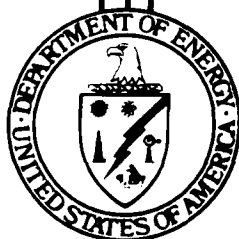


MICROCOPY RESOLUTION TEST CHART  
NATIONAL BUREAU OF STANDARDS-1963-A

ENERGY

DOH-HAK-THOZOO

NTIC FILE COPY



TRANSFORMATION TOUGHENED CERAMICS - A POTENTIAL  
MATERIAL FOR LIGHT DIESEL ENGINE APPLICATIONS

T. Y. Tien

June 1984

MATERIALS AND METALLURGICAL ENGINEERING  
THE UNIVERSITY OF MICHIGAN  
ANN ARBOR, MICHIGAN 48109

Final Report - 1 October 1982 to 30 September 1983

Contract DAAG46-82-C-0080

Approved for public release; distribution unlimited

Prepared for

ARMY MATERIALS AND MECHANICS RESEARCH CENTER  
Watertown, Massachusetts 02172

Under AMMRC/DOE Interagency Agreement EC-76-A-1017-002  
Department of Energy  
Office of Vehicle and Engine Research and Development  
Ceramic Technology for Advanced Heat Engines Programs

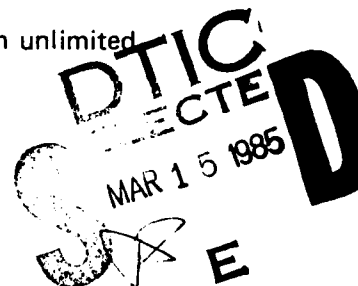
U.S. DEPARTMENT OF ENERGY  
Office of Vehicle and Engine Research and Development

85 03 06 002

2

AD

AMMRC TR 84-26



The findings in this report are not to be construed as an official Department of the Army position, unless so designated by other authorized documents.

Mention of any trade names or manufacturers in this report shall not be construed as advertising nor as an official indorsement or approval of such products or companies by the United States Government.

#### DISPOSITION INSTRUCTIONS

Destroy this report when it is no longer needed.  
Do not return it to the originator.

SECURITY CLASSIFICATION OF THIS PAGE (When Data Entered)

DD FORM 1 JAN 73 1473

SECURITY CLASSIFICATION OF THIS PAGE (When Data Entered)

UNCLASSIFIED

SECURITY CLASSIFICATION OF THIS PAGE (When Data Entered)

Block No. 20

## ABSTRACT

This report contains three parts: The thermal conductivity studies in the system  $\text{Al}_2\text{O}_3$ - $\text{Cr}_2\text{O}_3$ - $\text{ZrO}_2$ - $\text{HfO}_2$  are presented in the first part. The mechanical behavior of these compositions will be presented in the second part. The mullite -  $\text{ZrO}_2$  system will be discussed in the third part. The results indicate that a composition containing 15 mole % of  $\text{Cr}_2\text{O}_3$  in  $\text{Al}_2\text{O}_3$  in the matrix phase has a thermal conductivity comparable to that of stabilized zirconia.

Accession For	
NTIS GRA&I	<input checked="checked" type="checkbox"/>
DTIC TAB	<input type="checkbox"/>
Unannounced	<input type="checkbox"/>
Justification	
By	
Distribution/	
Availability Codes	
Avail and/or	
Dist	Special
A-1	



UNCLASSIFIED

SECURITY CLASSIFICATION OF THIS PAGE (When Data Entered)

THERMAL CONDUCTIVITY STUDIES  
IN THE SYSTEM  $\text{Al}_2\text{O}_3$ - $\text{Cr}_2\text{O}_3$ - $\text{ZrO}_2$ - $\text{HfO}_2$

S.K. Yu and T.Y. Tien  
Materials and Metallurgical Engineering  
The University of Michigan  
Ann Arbor, Michigan 48109

## I. SAMPLE PREPARATION

Solid solutions of  $\text{Al}_2\text{O}_3\text{-Cr}_2\text{O}_3$  and  $\text{ZrO}_2\text{-HfO}_2$  were prepared separately by mixing appropriate amounts of oxides in a ball mill and reacted at  $1350^\circ\text{C}$  for 24 hours. Solutionized powders were then ball milled for 43 hours and dried at  $110^\circ\text{C}$ . Specimens for conductivity tests were hot pressed at  $1600^\circ\text{C}$  for one hour in BN coated graphite dies under a pressure of  $30 \text{ MN/m}^2$ . After hot pressing, the samples were then oxidized in air at  $1350^\circ\text{C}$  for 2 hours.

The compositions tested are listed in terms of X and Y in Table 1 where X is the m/o chromia in alumina and Y is the m/o hafnia in zirconia. The dispersed phase volume fraction was kept constant at 15 v/o. In all cases, full density was achieved.

## II. THERMAL CONDUCTIVITY MEASUREMENTS

The thermal conductivity of the 22 samples in the alumina containing system were measured by a 'comparative method'. The thermal conductivity is defined by

$$q = kA (dT/dx)$$

where  $q$  is the heat flux,  $A$  is the specimen cross sectional area,  $T$  is the temperature,  $x$  is the distance between two points in the sample, and  $k$  is the thermal conductivity. A reference sample and an unknown sample with the same cross-sectional area were placed in the Comparative Thermal Conductivity Instrument. The thermal conductivity of the unknown sample can be calculated by  $\text{Al}_2\text{O}_3 - \text{Cr}_2\text{O}_3$  and  $\text{ZrO}_2 - \text{HfO}_2$  were attrition milled separately for four hours at 1000 RPM. These solid solutions were then



mixed with a binder and ball milled for 6-8 hours. The material was isostatically pressed at a nominal pressure of 124 MPa and sintered. The bar specimens for bend strength measurements were sintered at 1550°C for 30 minutes in air. The samples for indentation tests were sintered at two different temperatures. The low chromia samples (0, 2, and 5 m/o) were sintered at 1550°C for 30 minutes in air. The high chromia samples were packed in powder of the same composition and sintered at 1650°C for 30 minutes in air. This was done to prevent chromia volatilization. The bars were machined to nominal dimensions of 5 cm x 0.22 cm x 0.21 cm. The samples for indentation tests were rough ground on 45-15 um diamond imbedded wheels and polished using 6 um and 1 um diamond impregnated lapping wheels. Twenty-four compositions of this system were tested with chromia contents (X) varying from 0-30 mole percent and hafnia content (Y) varying from 0-30 mole percent.

A Tukon Microhardness Testing Machine was used for the micro-hardness and indentation fracture toughness studies. A minimum of 5 indentations were made at each of 4 or more different loads for each sample. The load was varied from 3 to 10 kg. A Vickers diamond indenter (136°) was used in all studies.

Bend strength tests were performed on a closed-loop servo-hydraulic test machine with a 5000 N load cell. A four-point bending jig was used with a loading rate of  $8.5 \times 10^{-4}$  mm/sec. using the equation

$$(\Delta T/\Delta x)_{\text{unknown}} = (\Delta T/\Delta x)_{\text{reference}}$$

and by measuring  $\Delta T$  and  $\Delta x$  for the unknown and reference material.

The equipment used for these measurements is a commercial unit manufactured by Dynatech Corporation, model TCFCM Comparative Thermal

Conductivity Instrument. Measurements were made at 70, 250, and 400°C for all specimens. A schematic diagram of this equipment (1) is shown in Figure 1.

Twenty-two compositions in the system alumina-chromia-zirconia-hafnia were studied. Specimens for these measurements were hot pressed cylinders 3 cm in diameter and 2 cm in height. Both top and bottom surfaces were rough ground on 15  $\mu$ m diamond imbedded wheels.

### III. RESULTS

The results of the thermal conductivity measurements are shown in Table 1 and Figures 2-5. These data indicated that the thermal conductivity decreases with increasing chromia. The effect of hafnia on the thermal conductivity is negligible.

The data in Figure 2 (70°C) can be extrapolated back to 0% chromia. Assuming that the 10 m/o hafnia has little effect on the thermal conductivity, the value for pure zirconia in a pure alumina matrix would be 0.038 Cal/cm<sup>2</sup>°Csec. Claussen et al. (2) reported a thermal conductivity value for Al<sub>2</sub>O<sub>3</sub>-15v/oZrO<sub>2</sub> of 0.018 Cal/cm<sup>2</sup>°Csec at 70°C. The thermal conductivity values at 70°C can be normalized by multiplying by a factor of 18/38. The normalized data is shown in Figure 6. The normalized data indicate that the thermal conductivity of samples containing over approximately 15v/o chromia is below that of stabilized zirconia.

## REFERENCES

1. Operating Manual for the Model TCFCM Comparative Thermal Conductivity Instrument, Dynatech R/D Company, Cambridge, MA.
2. Greve, D., Claussen, N., Hasselman, D.P.H. and Youngblood, "Thermal Diffusivity/Conductivity of Alumina with a Zirconia Dispersed Phase", Am. Ceram. Soc. Bull. 56, (1977) 514-515.

Table 1. Thermal Conductivity Data (Cal/cm °C sec)

Sample No. X - Y	70°C	250°C	400°C
0-100	0.0399	0.0219	0.0156
0-0	0.0273	0.0177	0.0137
2-10	0.0378	0.0240	0.0182
2-20	0.0332	0.0180	0.0132
2-30	0.0348	0.0179	0.0120
2-50	0.0292	0.0197	0.0147
5-20	0.0274	0.0174	0.0133
5-30	0.0277	0.0164	0.0121
5-50	0.0274	0.0165	0.0127
10-10	0.0165	0.0125	0.0108
10-20	0.0241	0.0170	0.0138
10-30	0.0229	0.0144	0.0108
10-50	0.0233	0.0152	0.0118
20-10	0.0153	0.0105	0.0082
20-20	0.0179	0.0121	0.0094
20-30	0.0188	0.0137	0.0111
20-50	0.0191	0.0138	0.0110
30-10	0.0168	0.0122	0.0099
30-20	0.0156	0.0113	0.0093
30-30	0.0178	0.0139	0.0119
30-50	0.0177	0.0139	0.0119

X = the m/o chromia in alumina

Y = the m/o hafnia in zirconia

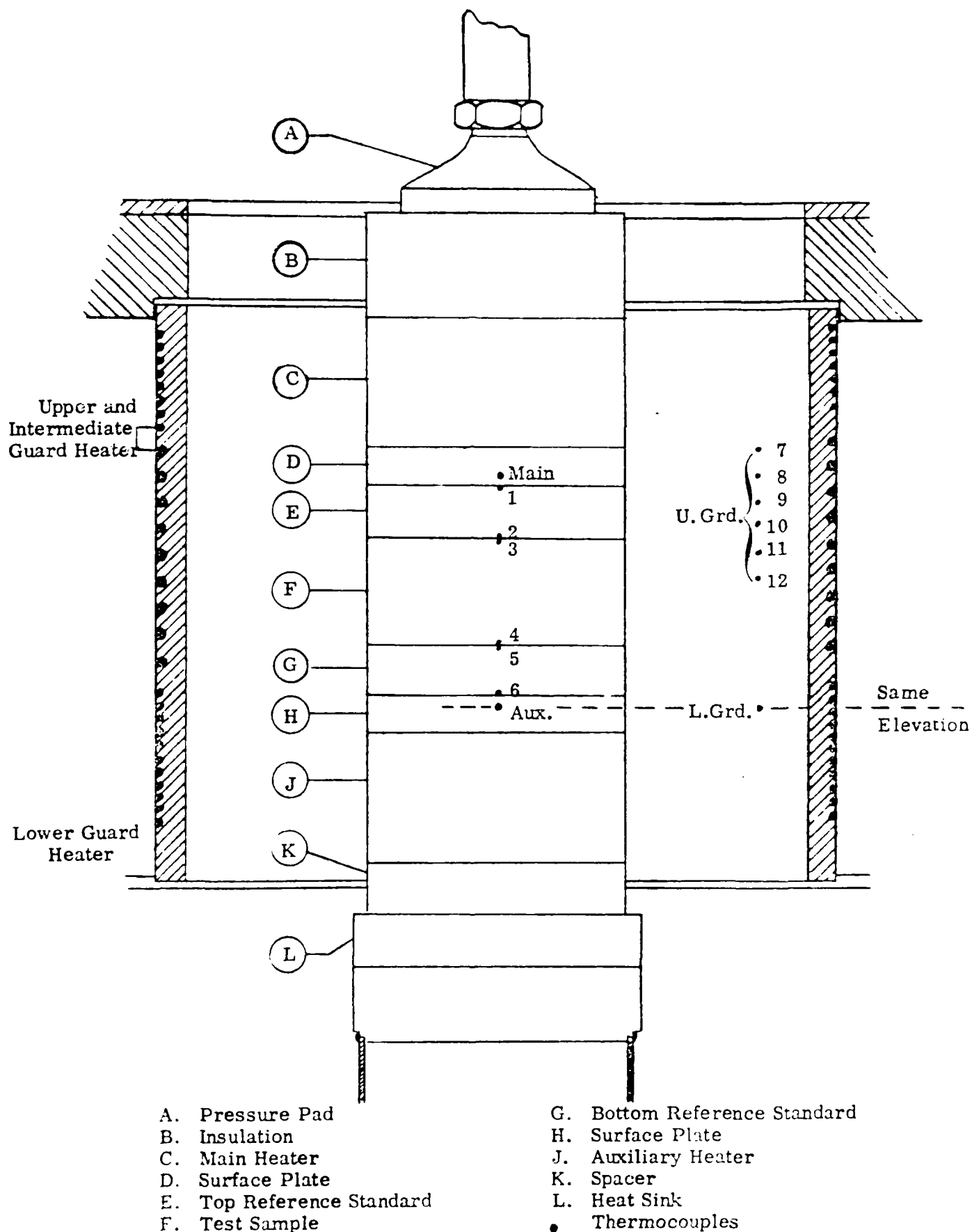


FIG. 1

TEST STACK FOR TESTS USING PYREX OR  
PYROCERAM REFERENCE STANDARDS (1)  
(2" or 2.5" dia. or squ.)

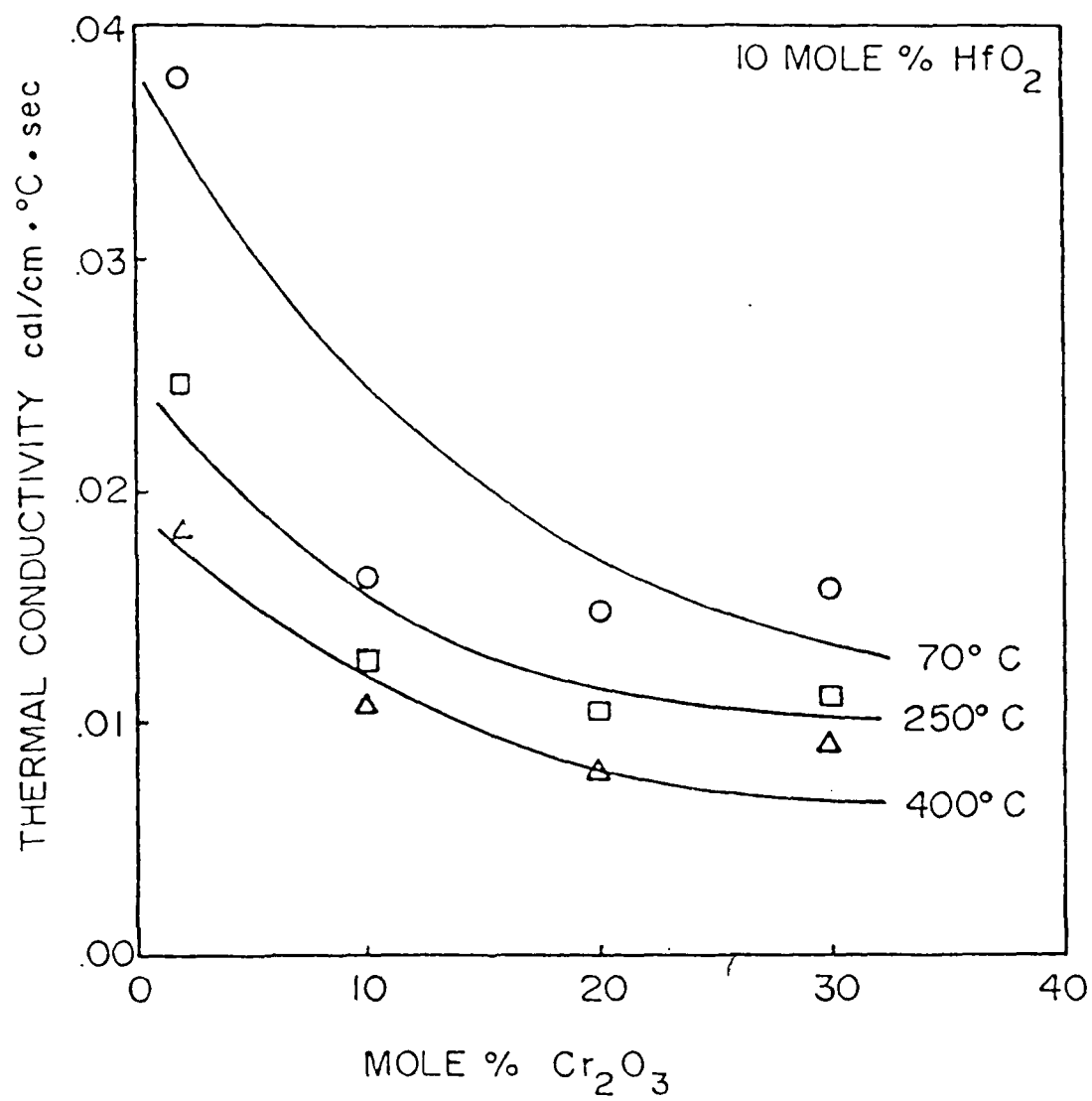


Fig. 2

most of this decrease can be attributed to thermal shock. Microstructural examination shows that the particle size did not change as a result of the ageing treatment. Hence, it appears that microstructural stability has been enhanced by chromia additions. Further studies are needed however to substantiate this condition.

## CONCLUSIONS

1. The decrease in bend strength with increasing chromia content can be attributed to porosity.
2. The critical particle size decreases with increasing hafnia content.
3. The fracture toughness generally increases with increasing hafnia content.
4. The fracture toughness generally increases with increasing chromia content.
5. Stress induced transformation is not the only mechanism for toughening in this material under these conditions.

## REFERENCES

1. Anstis, G.R., Chantikul, P., Lawn, B.R., and Marshall, D.B., "A Critical Evaluation of Indentation Techniques for Measuring Fracture Toughness: I. Direct Crack Measurements", J. Am. Ceram. Soc., 64, (1981), 533-538.
2. Hucke, E.E., "Process Development for Silicon Carbide Based Structural C Ceramics", Report DAAG46-80-c-0056-P0004, June 1982, Army Materials and Mechanics Research Center, Watertown, Massachusetts.
3. Engineering Property Data on Selected Ceramics, Vol. III, Single Oxides, MCIM-HB-07, Metals and Ceramics Information

Microcrack nucleation occurs when the tetragonal-to-monoclinic phase transformation causes the nucleation of microcracks in the material surrounding a particle. The nucleation of microcracks can occur as a sample is being cooled (spontaneous microcracking) or under an applied stress. In either event energy is converted to surface energy, not crack propagation, and the fracture toughness is increased. Transformation toughening by microcrack nucleation can only occur if monoclinic particles are present in the microstructure.

The amount of tetragonal phase present in the microstructure of each composition was compared with the fracture toughness of the material. These results are shown in Figure 13. These results appear to indicate that the percent tetragonal phase present in the material does not have much if any effect on the fracture toughness of the material. The slope of the best fit through these points is  $-.012$  with an intercept of  $5.129$  and a correlation coefficient of  $-.271$ . The conclusion that can be made from this data is that stress induced transformation toughening is not the only mechanism and probably not the controlling mechanism for toughening in this material for an average particle size of slightly less than  $1 \text{ } \mu\text{m}$ .

AGEING - Samples containing 2 m/o chromia and 20 m/o hafnia were heat treated for 602 hrs at 850, 1000, and 1150°C. After heat treating, the samples were removed from the furnace directly to room temperature. The samples were indented to measure the fracture toughness. Preliminary results show a decrease in the fracture toughness of approximately 20%. The authors feel that



this trend is not evident and at this time cannot explain these results. Figure 12 shows the relationship between the percent tetragonal phase and the hafnia content. The percent of tetragonal phase decreases with increasing hafnia content. Increasing hafnia additions to  $\text{ZrO}_2$  will decrease the critical particle size for the tetragonal-to-monoclinic phase transformation (7). If the particle size distribution is the same for all the compositions then the percentage of retained tetragonal phase will decrease with increasing hafnia content agreeing with our results. Preliminary investigations show that the particle size distribution is the same for the low chromia and high chromia samples even though the sintering temperatures were different.

Several toughening mechanisms in these and similar materials have been studied, all of which may or may not contribute to the fracture toughness of the alumina-chromia/zirconia-hafnia system. Among these, stress induced transformation toughening, toughening by microcrack nucleation, and toughening by crack/particle interaction are three mechanisms that are of great interest. Stress induced transformation toughening can only occur if tetragonal particles are present in the microstructure. When a material containing tetragonal phase particles is under an applied stress, these particles may transform to the monoclinic phase. This transformation and the volume expansion associated with it exerts a compressive stress around the crack tip. This compressive stress will inhibit crack extension and increase the fracture toughness.

transformation temperature and increasing the chemical driving force for the tetragonal-to-monoclinic phase transformation. The results presented here tend to agree with this theory.

Results from an earlier study (Figures 9 and 10) do not show similar trends. Here samples were hot pressed and the average  $\text{ZrO}_2$  particle size was about 5  $\mu\text{m}$ . This is approximately 5-10 times the critical particle size for the tetragonal-to-monoclinic phase transformation. The average  $\text{ZrO}_2$  particle size of the sintered materials in our present work is slightly less than 1  $\mu\text{m}$ . The hot pressed fracture toughness data is presented here only to show that comparable fracture toughness values can be attained in sintered materials by reducing the particle size by a factor of 5 to a size at or below the critical particle size.

**TOUGHENING MECHANISMS** - In an attempt to determine the toughening mechanism in these materials the amount of tetragonal phase was determined by using X-ray diffraction with the necessary corrections as reported by Porter and Heuer (8). The amount of tetragonal phase can be estimated by measuring the peak heights of the (111) tetragonal peak and the (11 $\bar{1}$ ) monoclinic peak and using the equation,

$$\% \text{Tet} = (111)_T / ((111)_T + 1.603(11\bar{1})_M)$$

The data obtained is shown in Figures 11 and 12. The percentage of retained tetragonal phase decreases with increasing chromia content. Ignoring nucleation and growth phenomena one would expect the percentage of retained tetragonal phase to increase with an increase in the modulus of the material (9). However,

all compositions.

**FRACTURE TOUGHNESS** - The results of the fracture toughness tests are shown in Figures 7 and 8. The effect of chromia on the fracture toughness are shown in Figure 7. With constant hafnia content, the fracture toughness increases with increasing chromia content. This could in part be due to an expected increase in the modulus of elasticity of the material. The effect of chromia shown here may even be underestimated by these results. A modulus of elasticity value must be used to calculate the fracture toughness using the equation above. The modulus of elasticity was not measured in this study and was assumed constant for our calculations. The data reported by Rossi and Lawrence (5) suggests that a peak occurs in the modulus of elasticity versus chromia content curve between 5 and 15 v/o chromia. However, their data is limited and not well enough defined to correct for modulus of elasticity changes. In addition, if increasing the chromia content increases the modulus of elasticity, not only are these trends underestimated but also the fracture toughness values calculated should be conservative as well.

The effect of hafnia content on the fracture toughness is shown in Figure 8. Withoug chromia, the fracture toughness decreases with increasing hafnia content. At present, no explanation is offered for these results. For all other chromia contents, an opposite effect is seen. With constant chromia content, the fracture toughness increases with increasing hafnia content. It is well known (6,7) that hafnia additions to  $ZrO_2$  increases the potential for toughening by increasing the

general trend of these results show that the average bend strength decreases with chromia content. This behavior can be explained by the data presented in Figure 2 which shows that the density of the bars also decreases with chromia content. From the preliminary data, it appears that the bend strength degradation can be attributed to porosity and that compositional effects are greatly overshadowed by this effect. The data shown in Figure 3 further supports this. The bend strength versus porosity data suggests that, for these bars, the bend strength is dependent on density and is independent of composition. Further evidence of high porosity is shown in Figure 4. This photomicrograph was taken on the fracture surface of a bar containing 20 m/o chromia. There is no evidence of any transgranular cracking and many areas that are not sintered. The fracture surface of a bar containing no chromia is shown in Figure 5. In this sample there is much more transgranular cracking, much less porosity, and a higher bend strength. Figure 6 shows the maximum bend strength data versus composition. Again, the compositional effects on the bend strength are probably not seen due to porosity effects. But this data does suggest that bend strength values of approximately 500-600 MPa can be attained for low chromia containing material. These values can probably be improved with increasing chromia and higher densities. There also appears to be little effect of the hafnia content on the average or maximum bend strength. Preliminary results show that the grain size of the matrix and the dispersed phase particle size was approximately the same for

yield a straight line with a slope given by:

$$\text{slope} = \text{constant } (E/H)^{1/2}/K_{IC}.$$

By rearranging, the fracture toughness,

$$K_{IC} = \text{constant } (E/H)^{1/2}/\text{slope},$$

can be calculated.

The hardness (H) is determined from the  $a^2$  versus P curve where a is 1/2 the diagonal of the indentation. From Huccke's work (2), this hardness,  $H_0$ , is independent of load and is the hardness at large loads. The equation used to calculate this value was:

$$H_0 = k/s'$$

where k is a dimensionless constant for a Vickers diamond indenter ( $136^\circ$ ) and is equal to 4636. The slope,  $s'$ , is determined from the  $a^2$  versus P curve. The value of the constant in the first equation is of little significance since a standard was used for all of the calculations.

To determine  $K_{IC}$  the value of the elastic modulus, E, must be determined. A value of 41,340 MPa was used (3) and assumed constant for these calculations.

Plots of  $a^2$  versus P and  $c^{3/2}$  versus P curves were constructed for all indentation test data generated. The degree of linear fit was excellent ( $r^2 = .99$ ) for all the  $a^2$  versus P curves. The linear fit was good (for most tests  $r^2 > .96$ ) for the  $c^{3/2}$  versus P curves.

## RESULTS AND DISCUSSION

**BEND STRENGTH** - The results of the four point bending tests for the 24 different compositions are shown in Figure 1. The

The load versus crosshead displacement curves were plotted to measure the load at fracture.

#### DATA ANALYSIS

**BEND STRENGTH** - Bend strength values were calculated using the formula (2)

$$\sigma_b = (6Pa/bd^2)$$

where  $P$  = load/2,  $a$  = distance from the center of a load pin to the center of the nearest support pin,  $b$  = specimen width, and  $d$  = specimen height. Both the average bend strength and maximum bend strength values are included in this report. The average bend strength values represent the average of at least 4 different tests.

**FRACTURE TOUGHNESS** - Indentation testing has become a viable technique for establishing relative fracture toughness data and, in some special cases, absolute fracture toughness values. The technique of using an indenter to produce cracks at the corners of an indentation was used to measure the relative fracture toughness of alumina-chromia/zirconia-hafnia specimens. The equation used to calculate these materials properties was developed by Anstis et al. (1), which relates a material-independent constant to the fracture toughness, hardness, elastic modulus, crack size, and the applied load. A  $c^{3/2}$  versus  $P$  plot using the equation:

$$\text{constant} = (K_{IC} (H/E)^{1/2}) / (P/c^{3/2})$$

where  $c$  is the crack length, and  $P$  is the applied load, should

## ABSTRACT

Strength and fracture toughness have been studied at room temperatures for the  $(\text{Al}_2\text{O}_3 + \text{XCr}_2\text{O}_3) + 15\text{v/o } (\text{ZrO}_2 + \text{YHfO}_2)$  systems for  $\text{Cr}_2\text{O}_3$  contents ranging from 0-30 mole percent in  $\text{Al}_2\text{O}_3$  and  $\text{HfO}_2$  contents ranging from 0-30 mole percent in  $\text{ZrO}_2$ . Preliminary results indicate that bend strength is more strongly influenced by processing defects than composition. It was found that fracture toughness increased with increasing  $\text{Cr}_2\text{O}_3$  and  $\text{HfO}_2$  additions. Further work is required to elucidate the mechanisms of toughening and the effect of composition and particle size.

## INTRODUCTION

In an effort to optimize the mechanical and physical properties of candidate ceramic materials for elevated temperature structural components a research program has been initiated to study the effects of composition and processing on such properties in the  $\text{Al}_2\text{O}_3/\text{ZrO}_2$  system. Matrix composition has been varied by  $\text{Cr}_2\text{O}_3$  additions while the transforming particle composition has been varied by  $\text{HfO}_2$  additions. The eventual goal of this project is to decrease the thermal conductivity and improve the thermal stability of the microstructure without sacrificing strength and toughness.

## MATERIALS AND EXPERIMENTAL PROCEDURE

The system  $\text{Al}_2\text{O}_3 - \text{XCr}_2\text{O}_3 + 15\text{v/o } (\text{ZrO}_2 - \text{YHfO}_2)$  was tested to determine the fracture toughness and strength by microhardness indentation tests and four-point bend tests. Solid solutions of

TRANSFORMATION TOUGHENING  
IN THE  $\text{Al}_2\text{O}_3$ - $\text{Cr}_2\text{O}_3$ / $\text{ZrO}_2$ - $\text{HfO}_2$  SYSTEM

BY

T.K. BROG, J.W. JONES AND T.Y. TIEN  
DEPARTMENT OF MATERIALS AND METALLURGICAL ENGINEERING  
THE UNIVERSITY OF MICHIGAN  
ANN ARBOR, MICHIGAN 48109



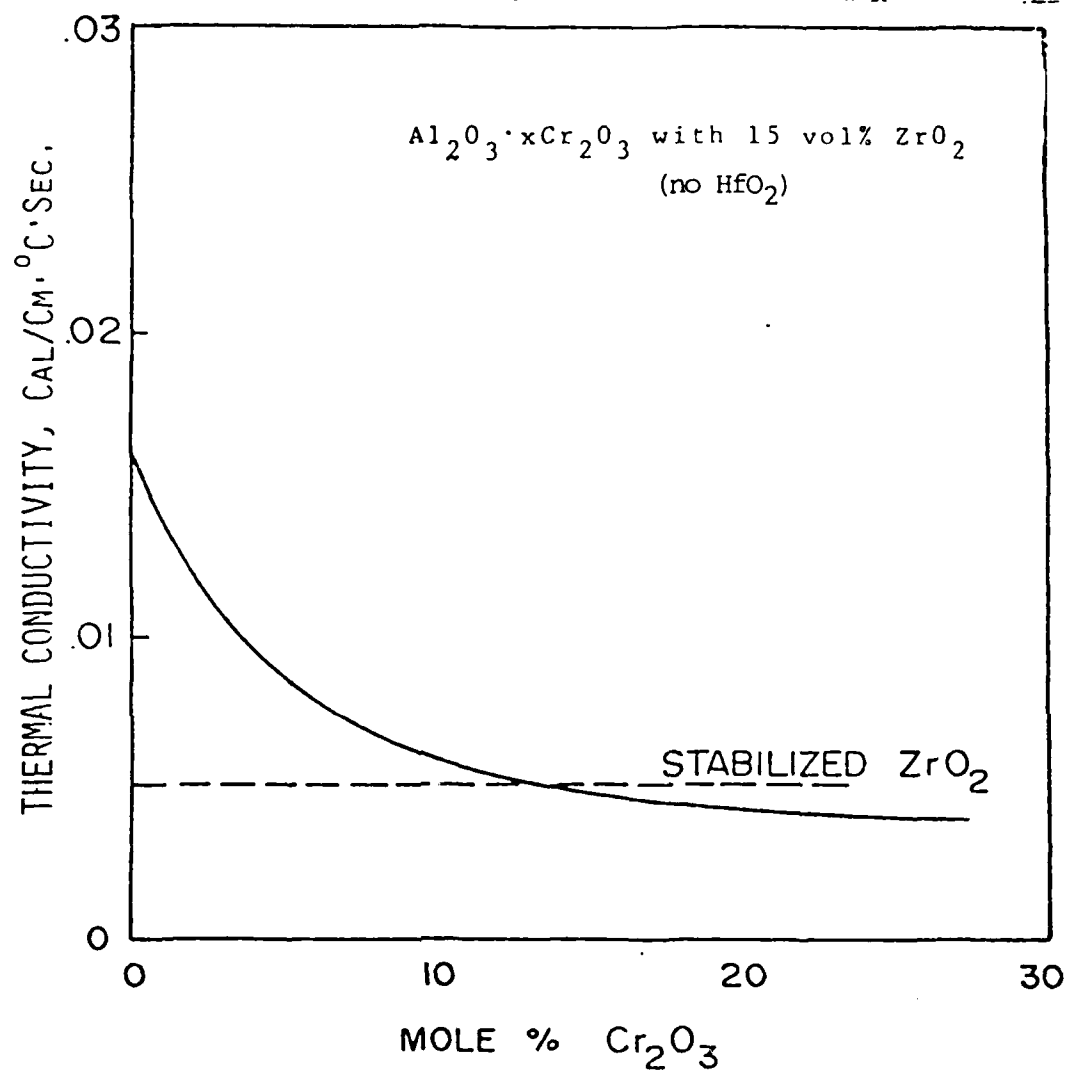


Fig. 6

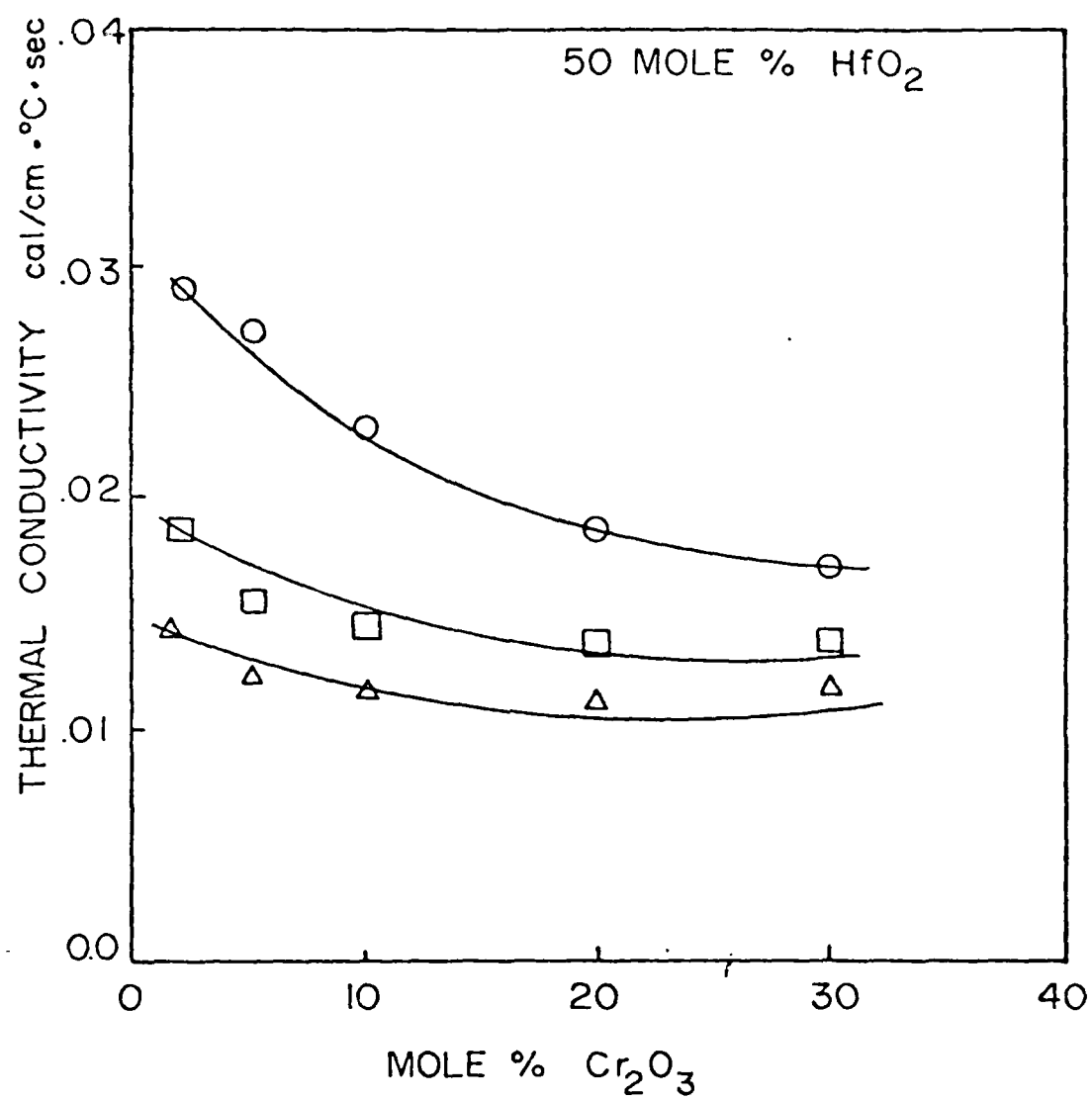


Fig. 5

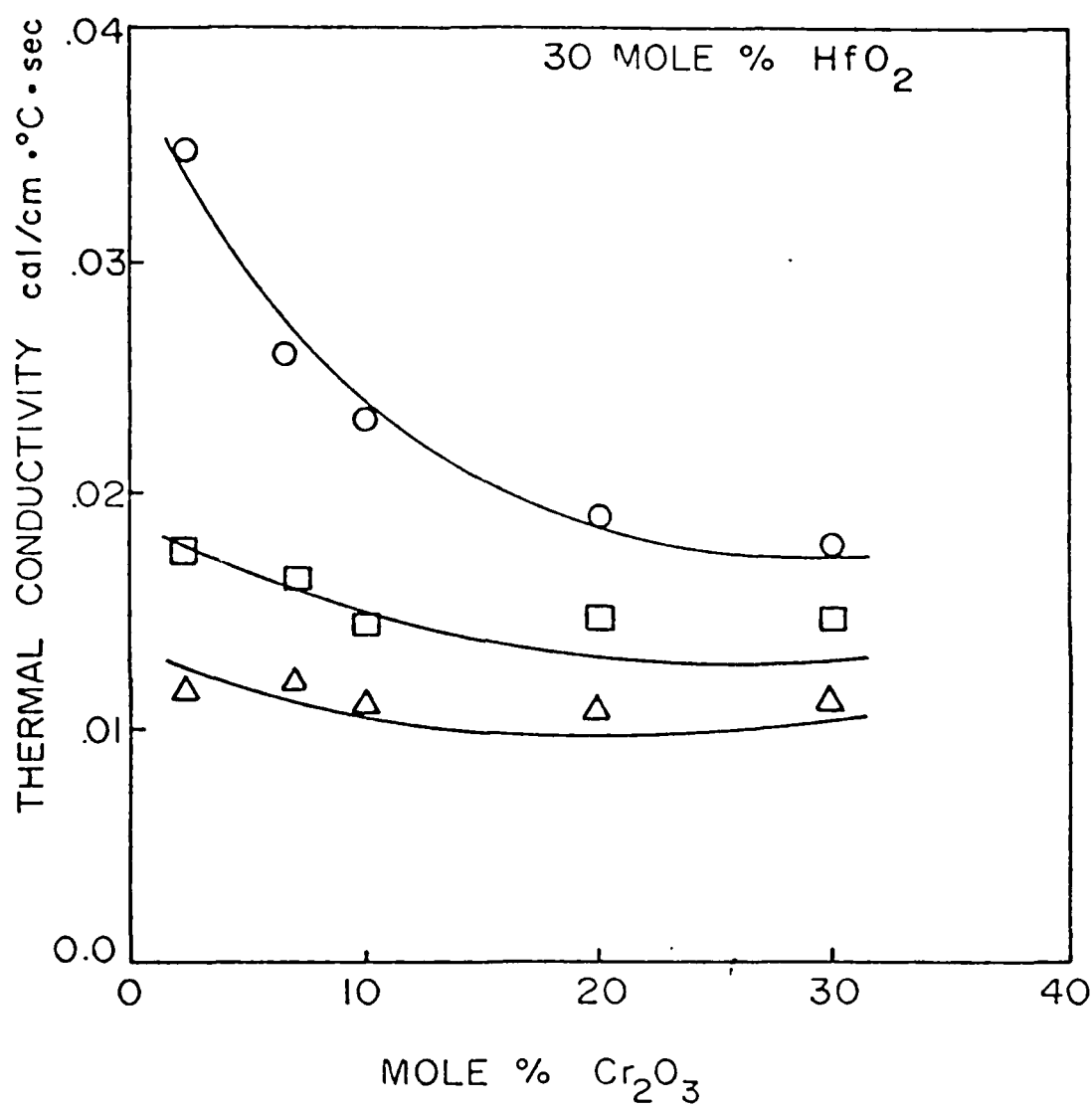


Fig. 4

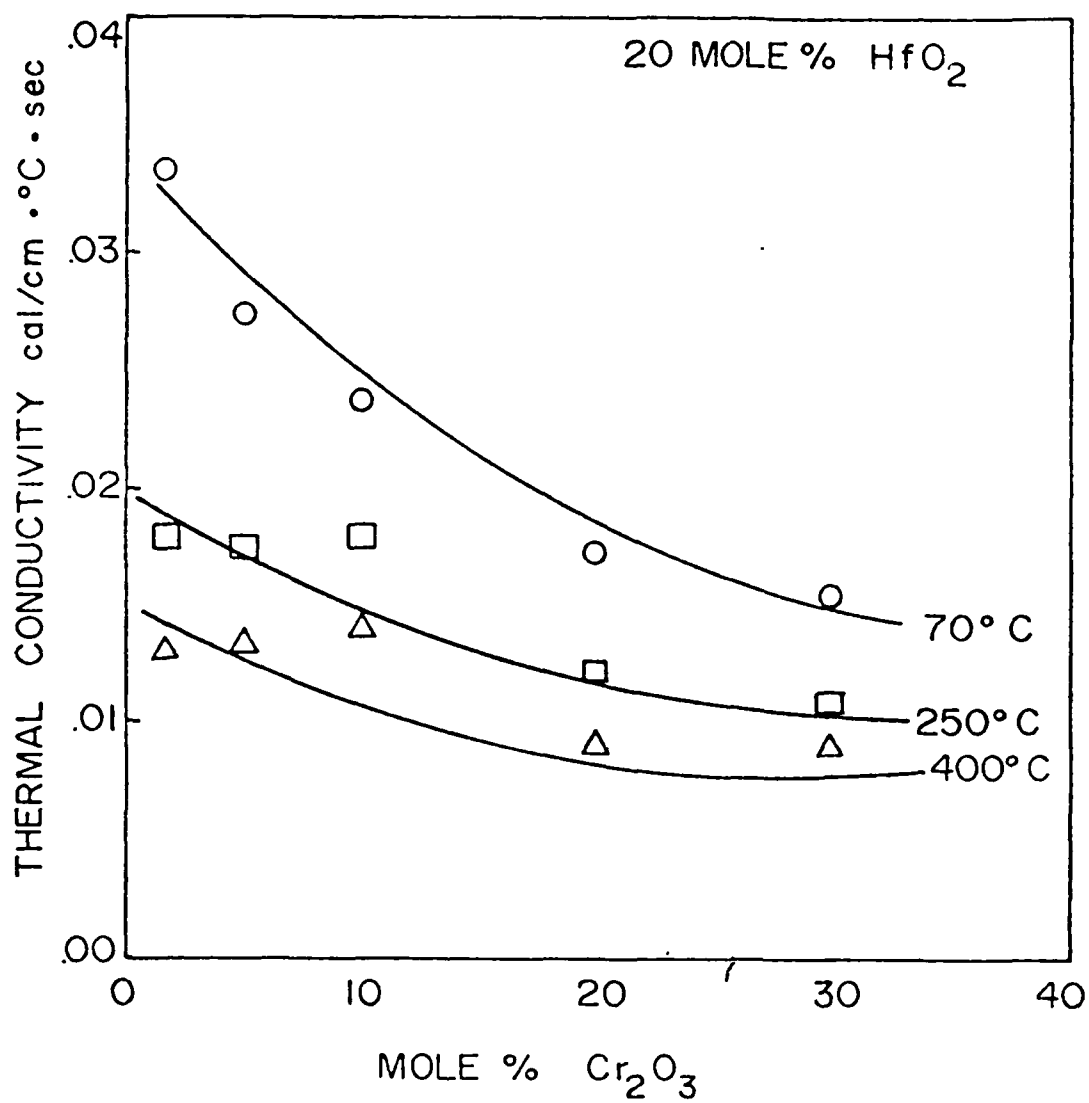


Fig. 3

Center, Battelle Memorial Institute, Columbus, Ohio,  
5.4.4-5.4.22.

4. Method T101, Flexure Test, Detailed Requirements, AMMRC.
5. Rossi, L.R., and Lawrence, W.G., "Elastic Properties of Oxide Solid Solutions: The System  $\text{Al}_2\text{O}_3 - \text{Cr}_2\text{O}_3$ ", J. Am. Ceram. Soc., 53, (1970), 604-608.
6. Claussen, N., and Ruhle, M., "Design of Transformation-Toughened Ceramics", Advances in Ceramics, The American Ceramic Society, Inc., Vol. 3, 1981, 137-164.
7. Claussen, N., Sigulinski, F., and Ruhle, M., "Phase Transformations of Solid Solutions of  $\text{ZrO}_2$  and  $\text{HfO}_2$  in an  $\text{Al}_2\text{O}_3$  Matrix", Advances in Ceramics, The American Ceramic Society, Inc., Vol. 3, 1981, 164-167.
8. Porter, D.L., and Heuer, A.H., "Microstructural Development in MgO - Partially Stabilized Zirconia (Mg-PSZ)", J. Am. Ceram. Soc., 62, (1979), 298-306.
9. Lange, F., "Transformation Toughening: Part 1 - Size Effects Associated with the Thermodynamics of Constrained Transformations", J. Mat. Sci., 17, (1982), 225-234.

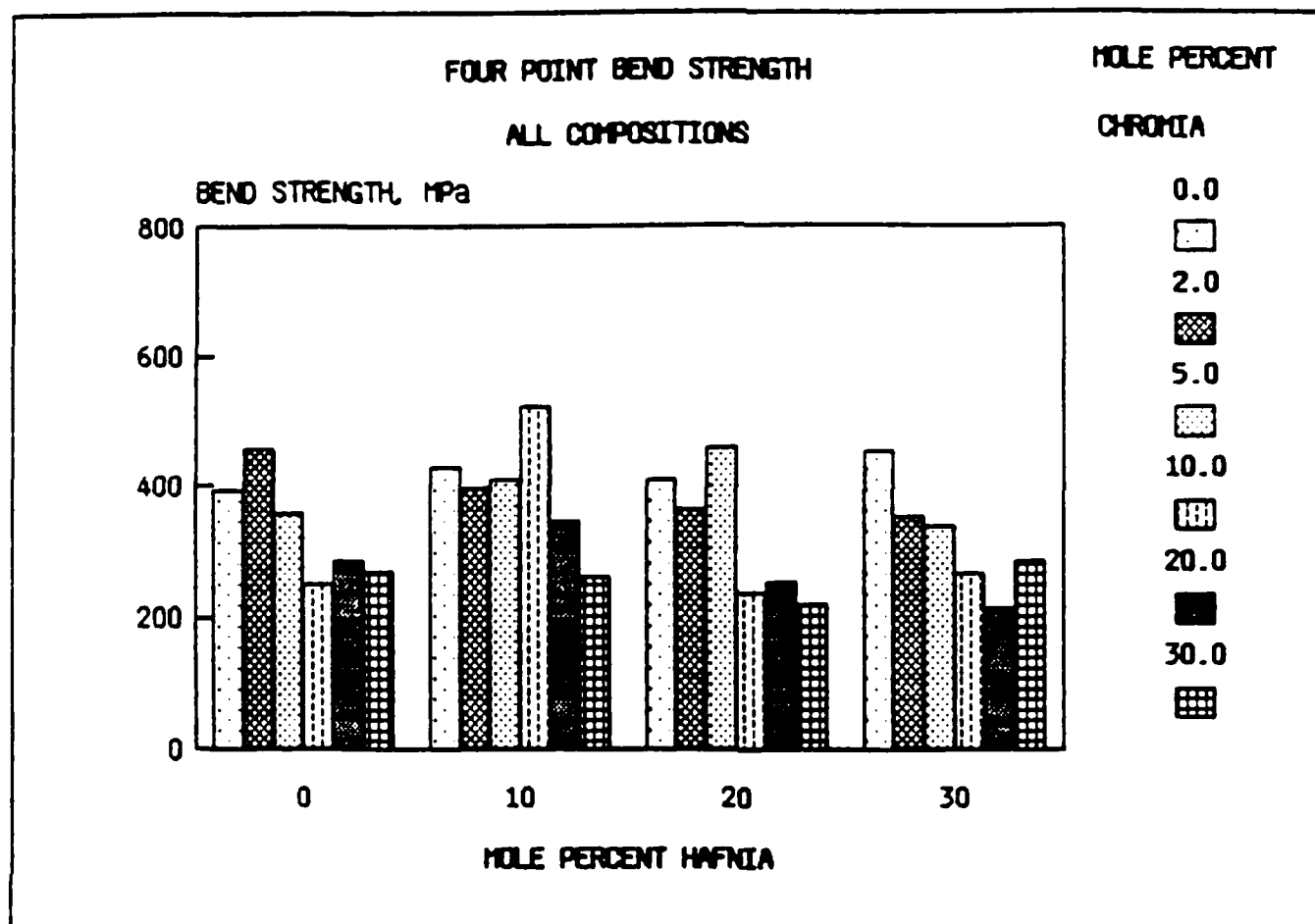


Figure 1. Bend strength versus chromia content for four different hafnia contents.

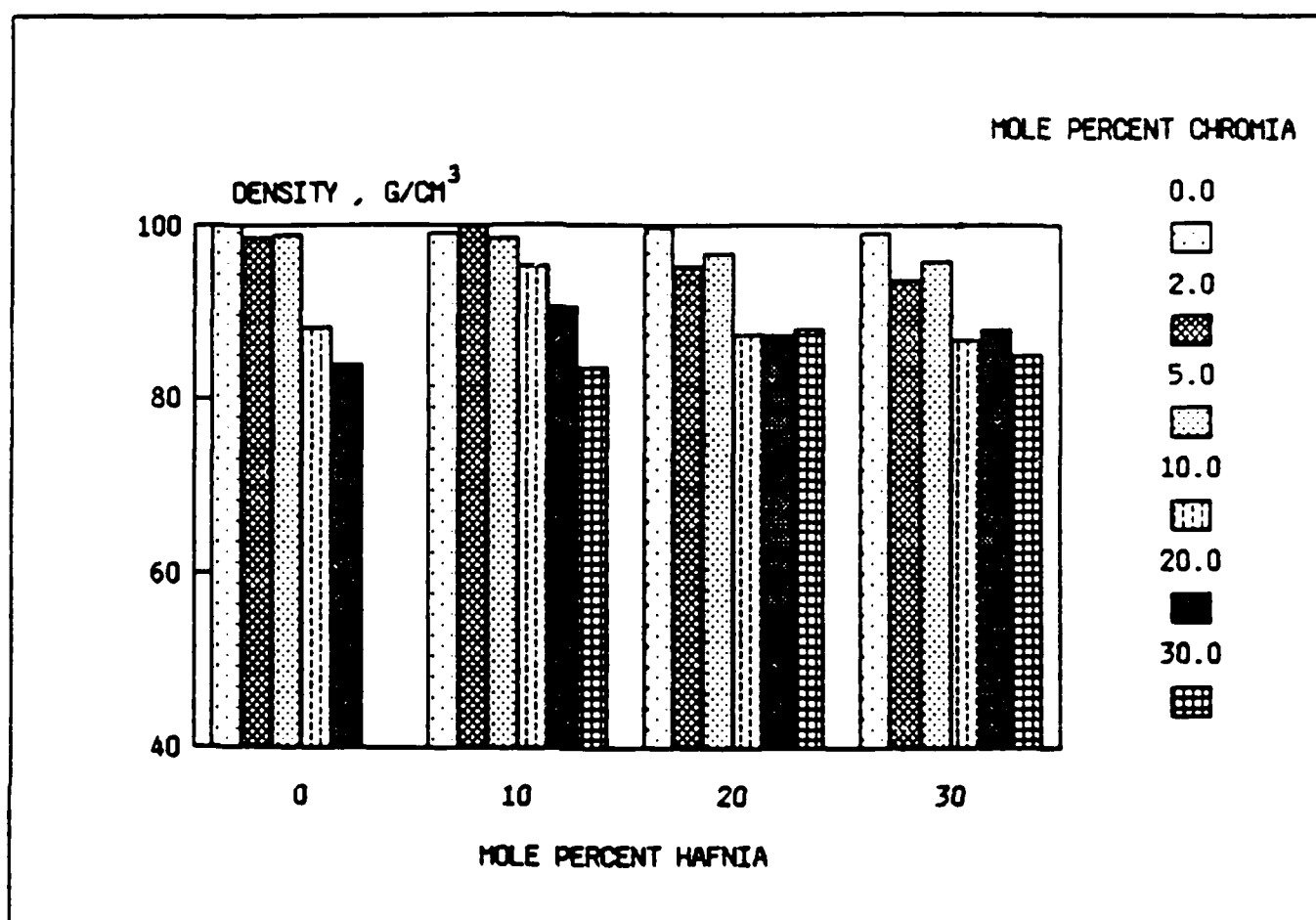


Figure 2. Density versus chromia content for four different hafnia contents.

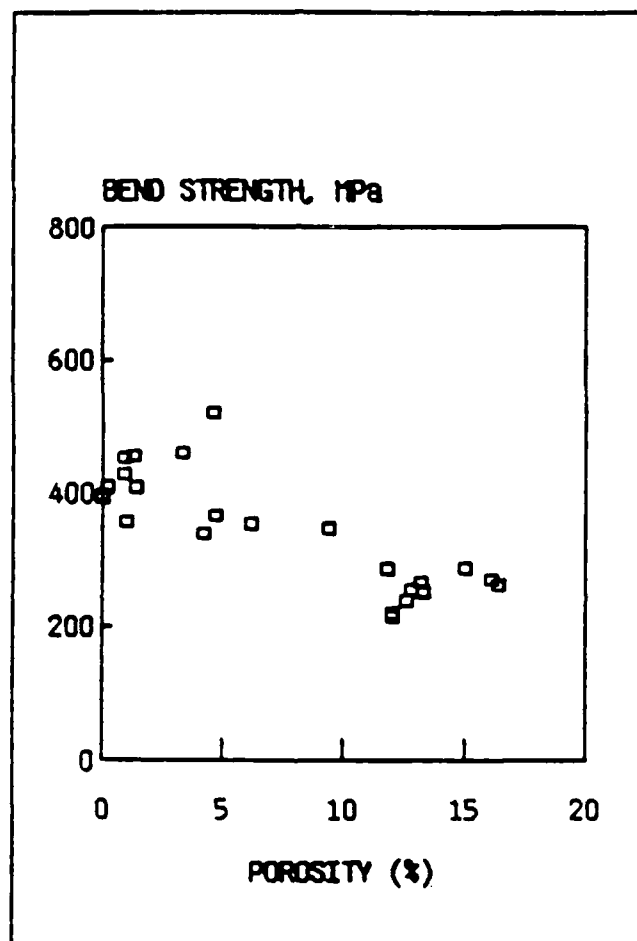


Figure 3. Bend strength versus porosity for 24 compositions of the  $\text{Al}_2\text{O}_3\text{-Cr}_2\text{O}_3$  /  $\text{ZrO}_2\text{-HfO}_2$  system.



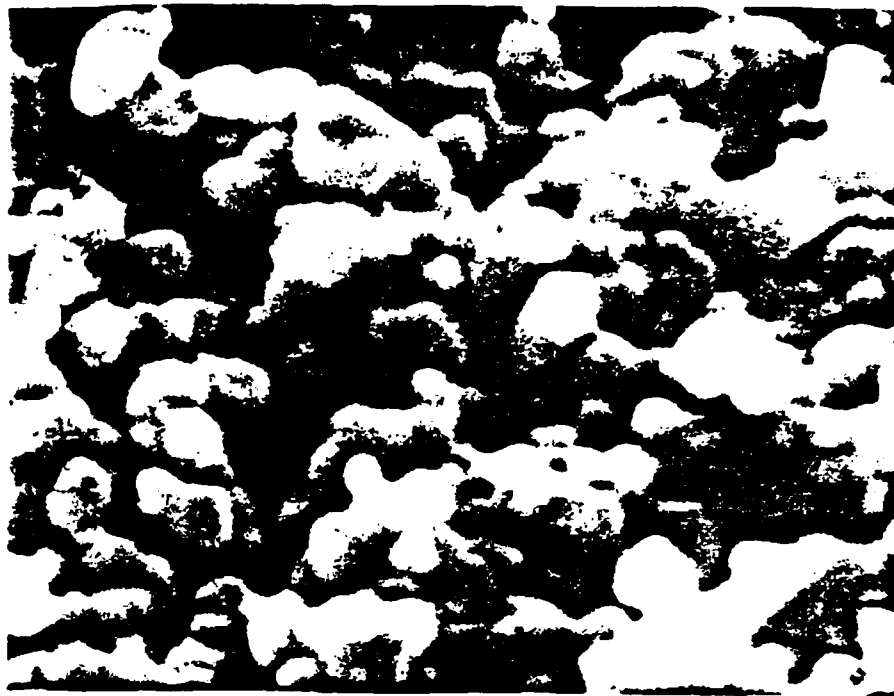



Figure 4. Fracture surface of 20 m/o chromia specimen fractured in bending. Note the lack of transgranular fracture and considerable porosity. SEM, 17.3 kx.  1μm

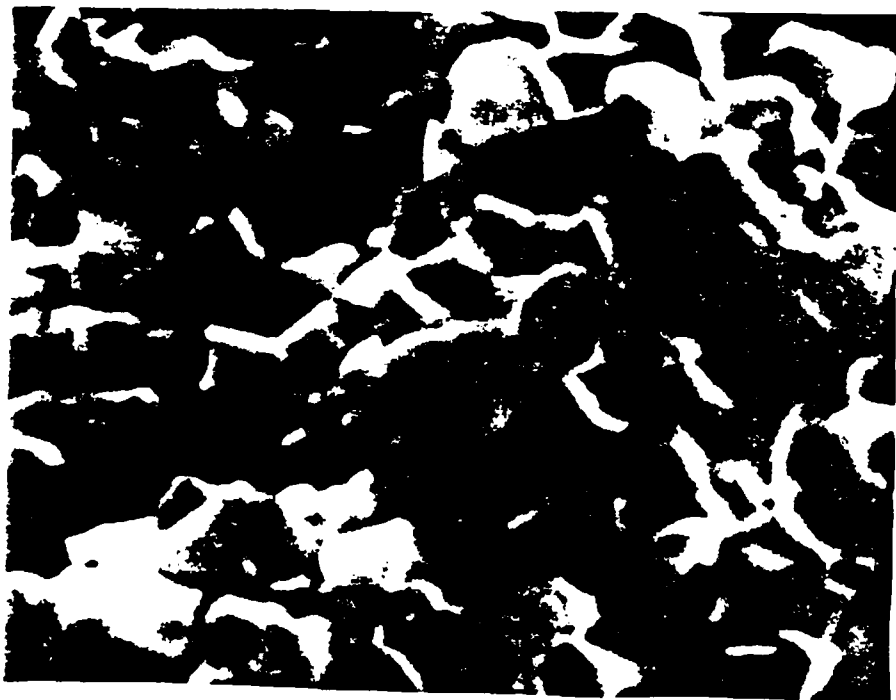



Figure 5. Fracture surface of bend specimen containing no chromia. Note decrease in porosity (compare with Fig. 4) and an increase in transgranular fracture.  1μm

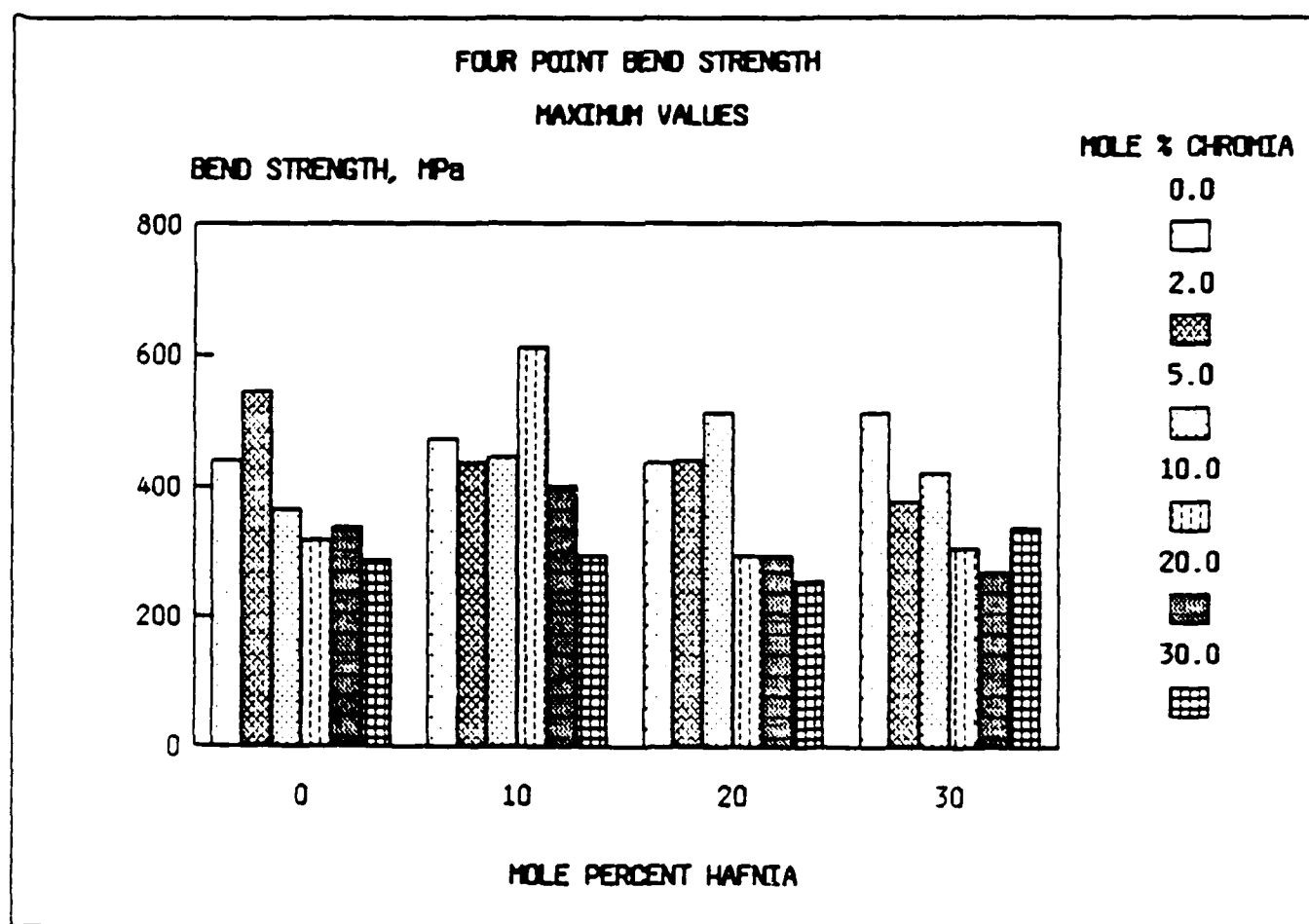


Figure 6. Maximum bend strength versus chromia content for four different hafnia contents.

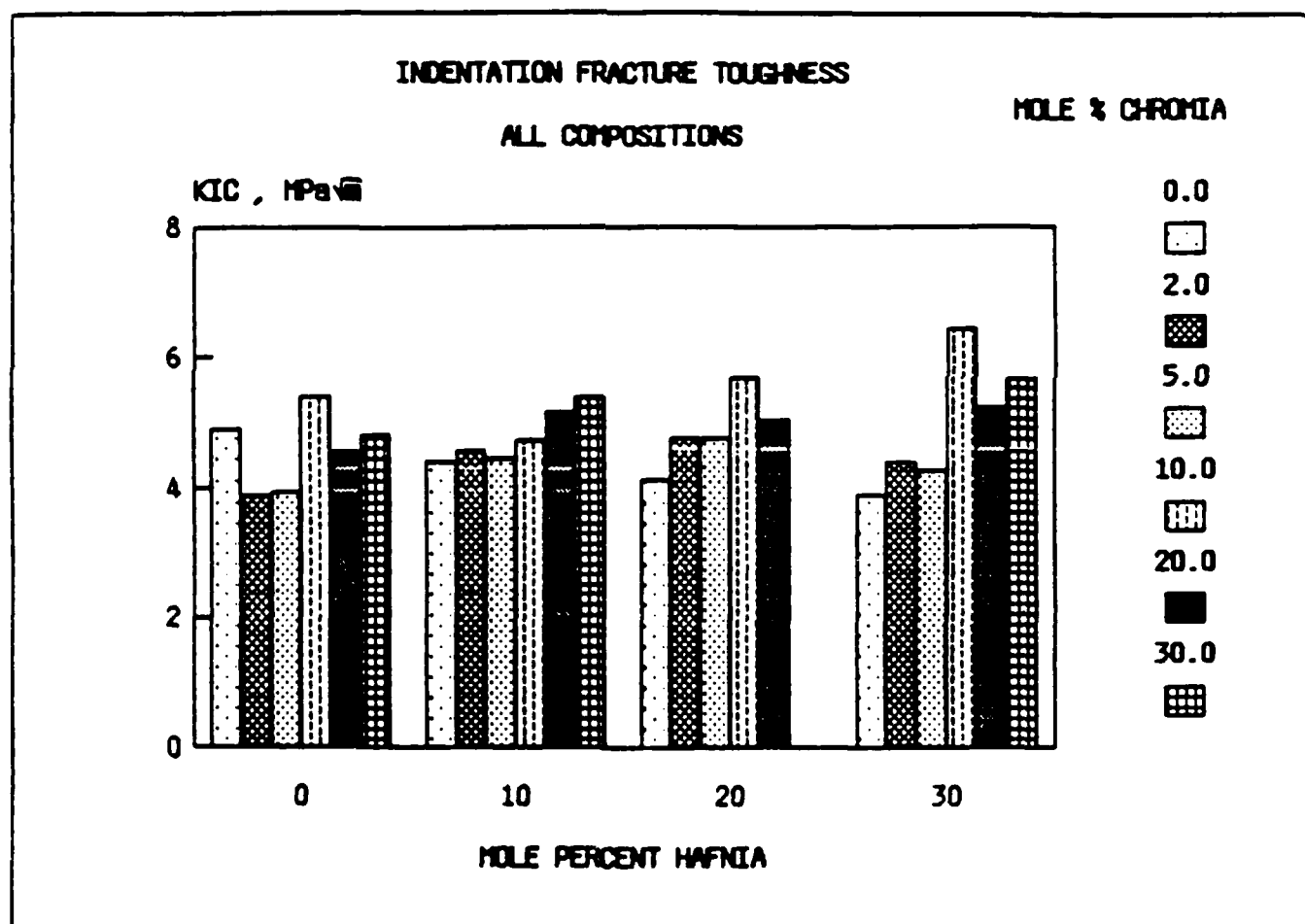


Figure 7. Fracture toughness versus chromia content of the sintered samples for four different hafnia contents.

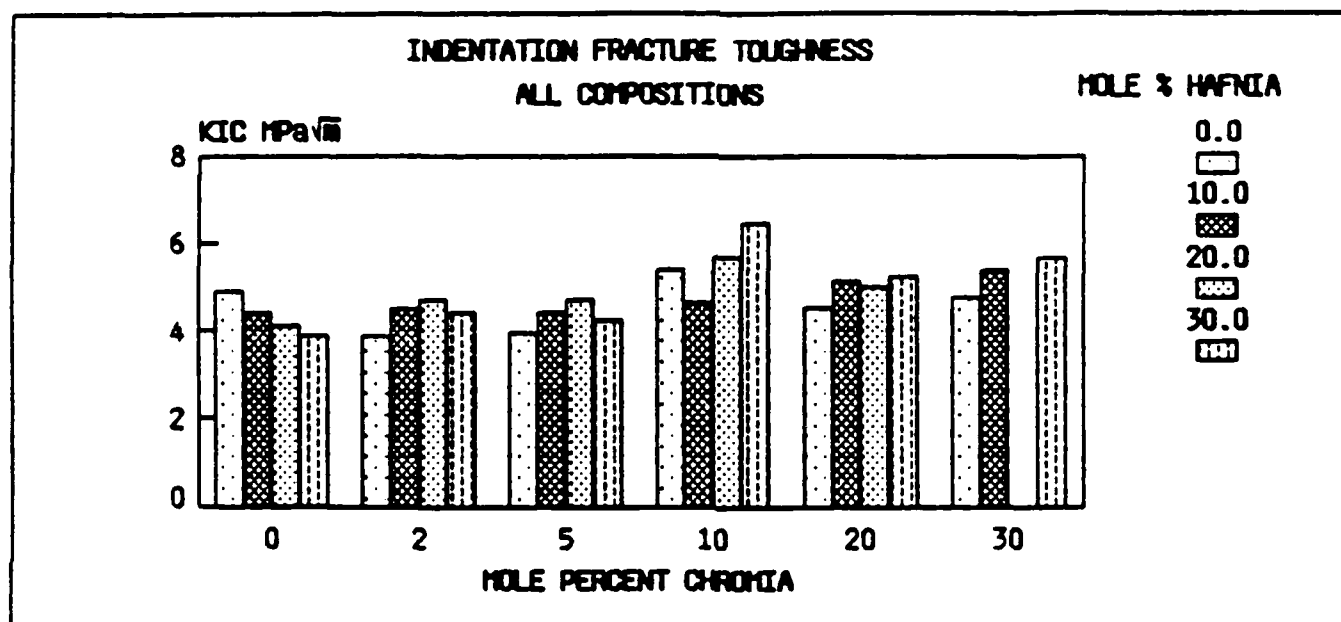


Figure 8. Fracture toughness versus hafnia content of the sintered samples for 6 different chromia contents.

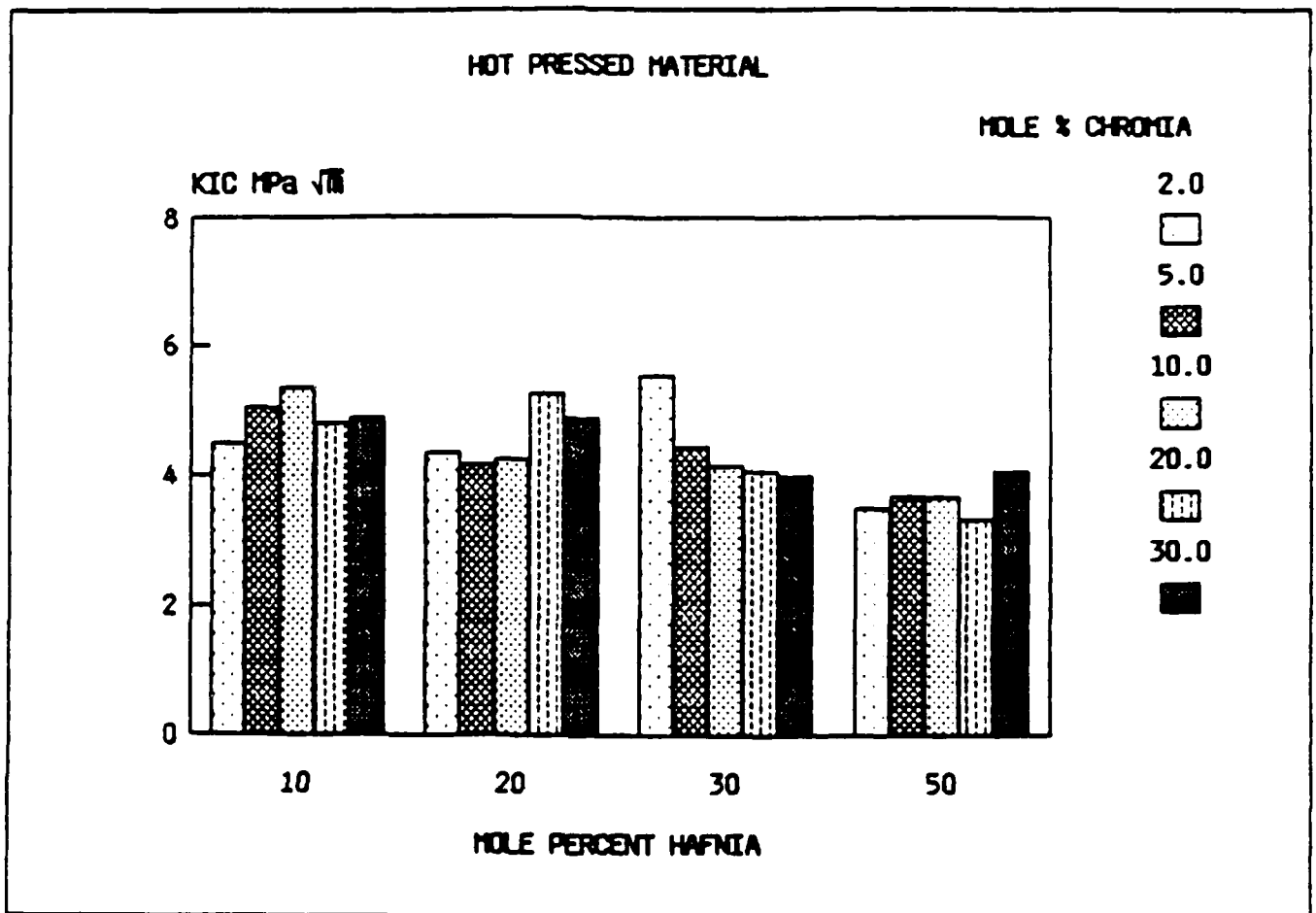


Figure 9. Fracture toughness versus chromia content of the hot pressed samples for four different hafnia contents.

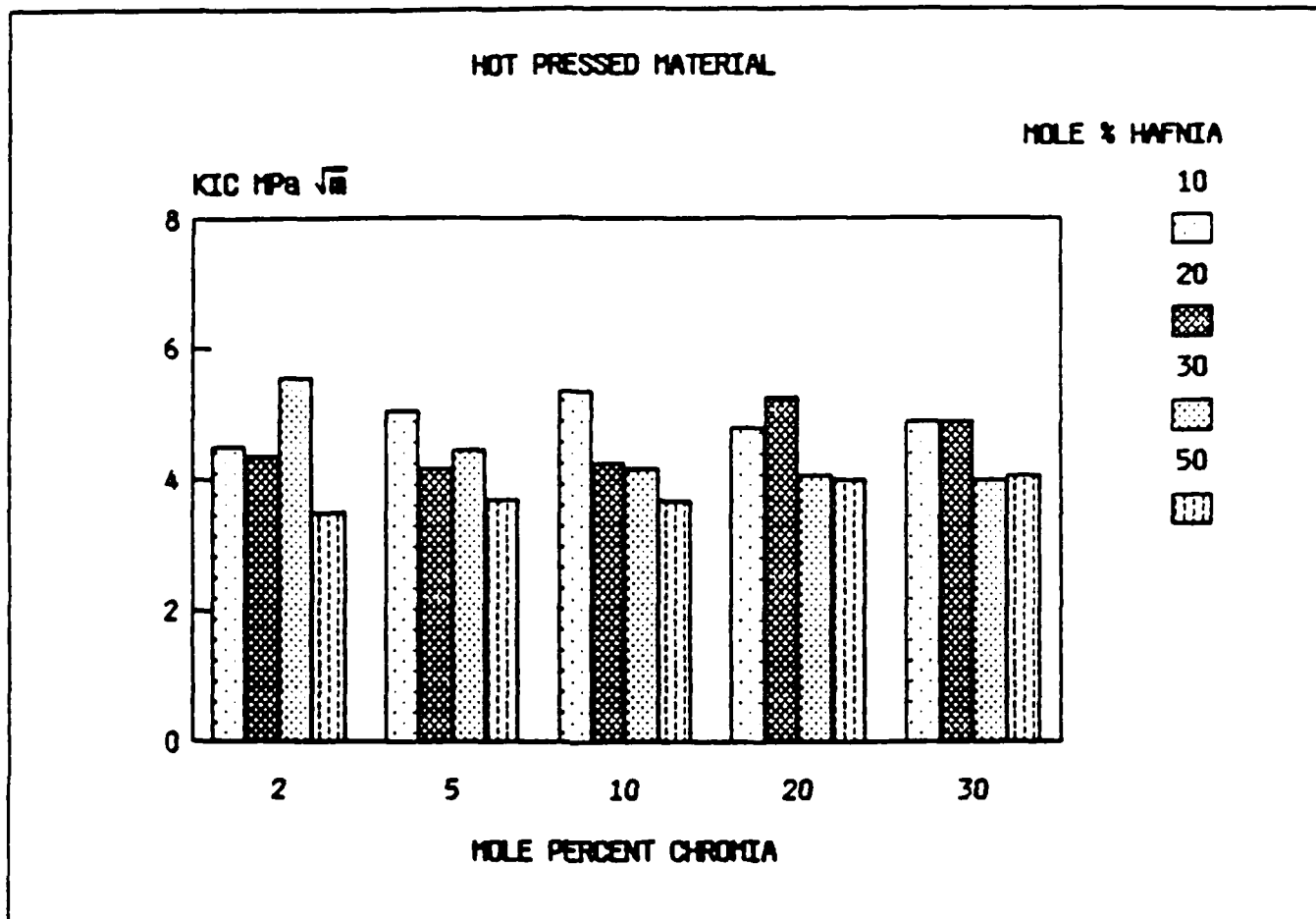


Figure 10. Fracture toughness versus hafnia content of the hot pressed samples for 6 different chromia contents.

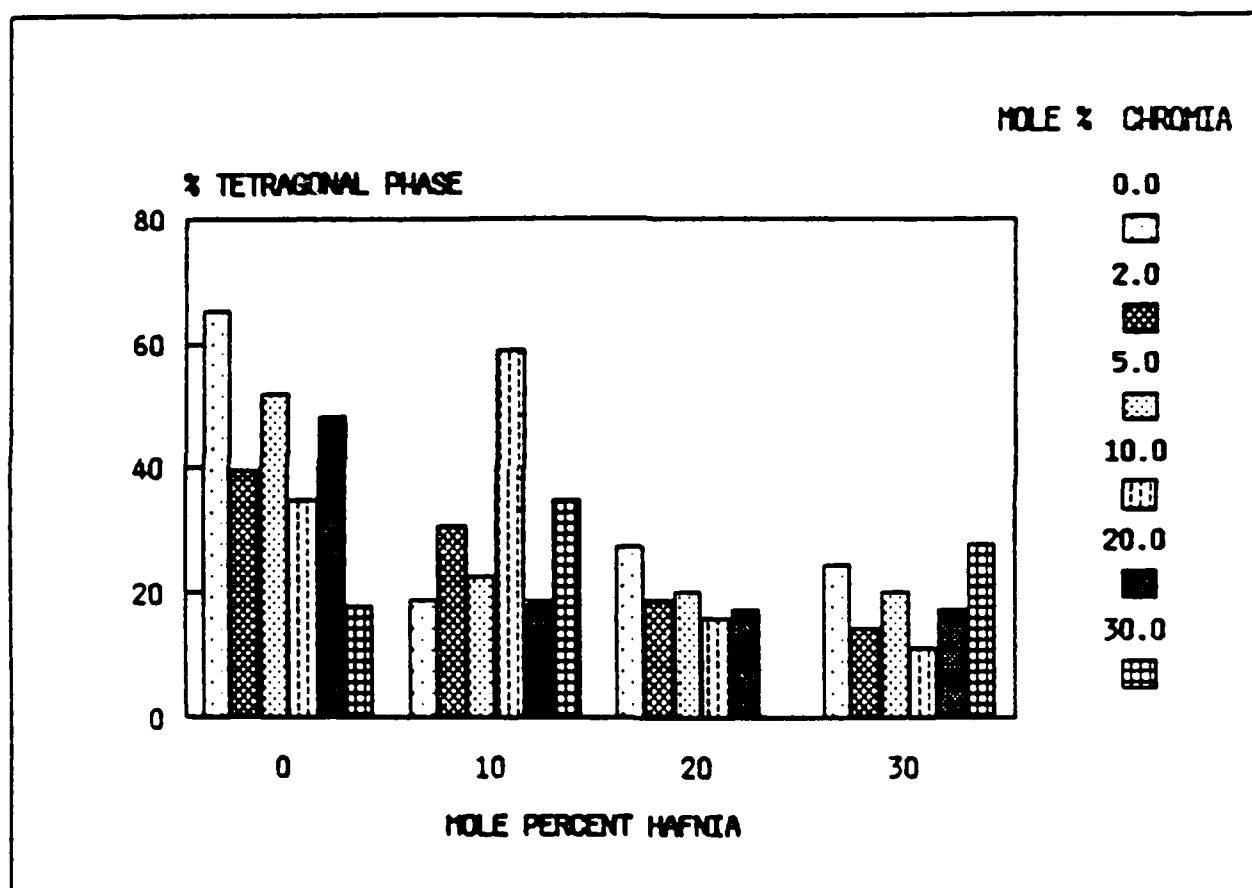


Figure 11. Percentage of tetragonal phase versus chromia content for four different hafnia contents.

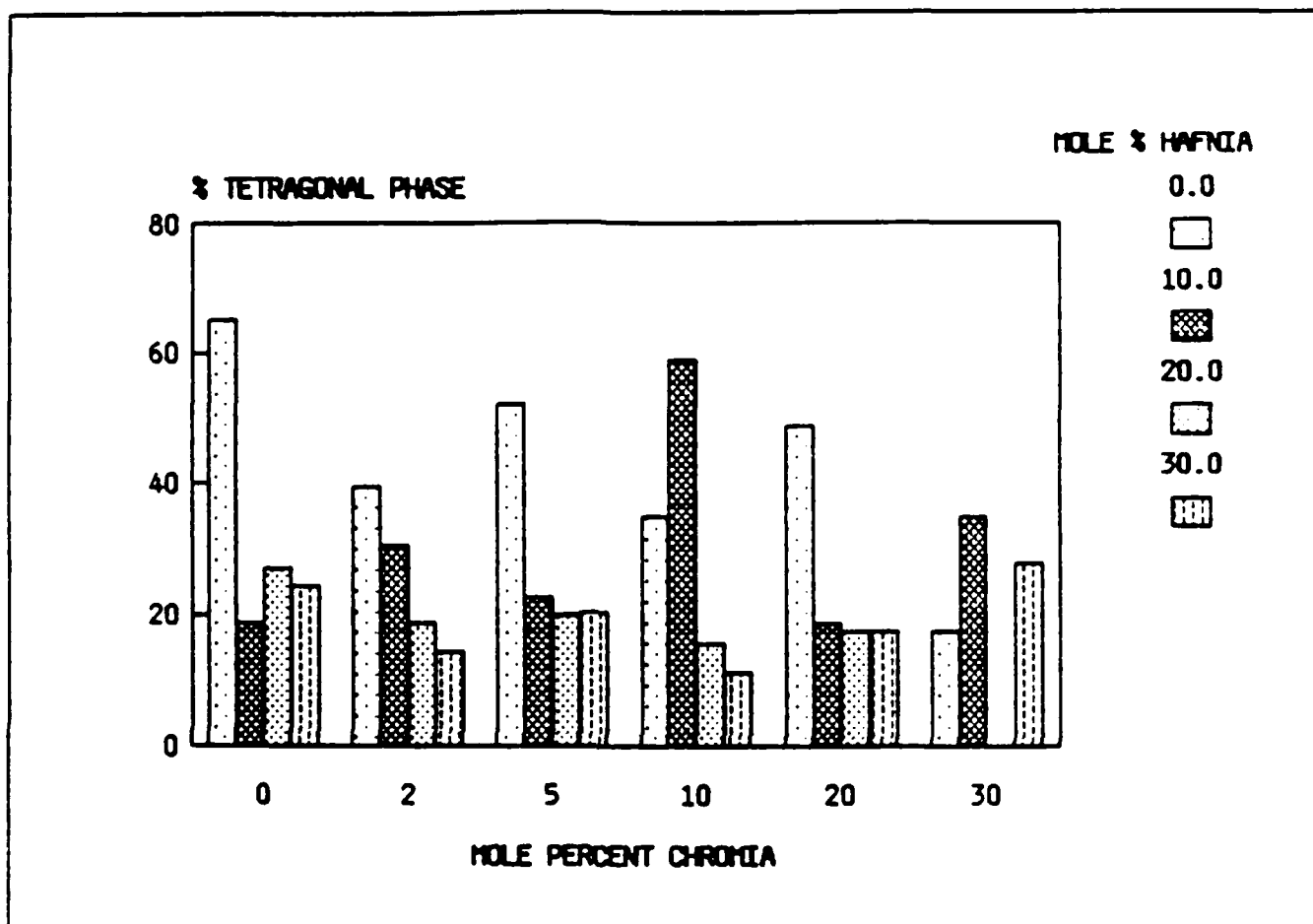


Figure 12. Percentage of tetragonal phase versus hafnia content for six different chromia contents.



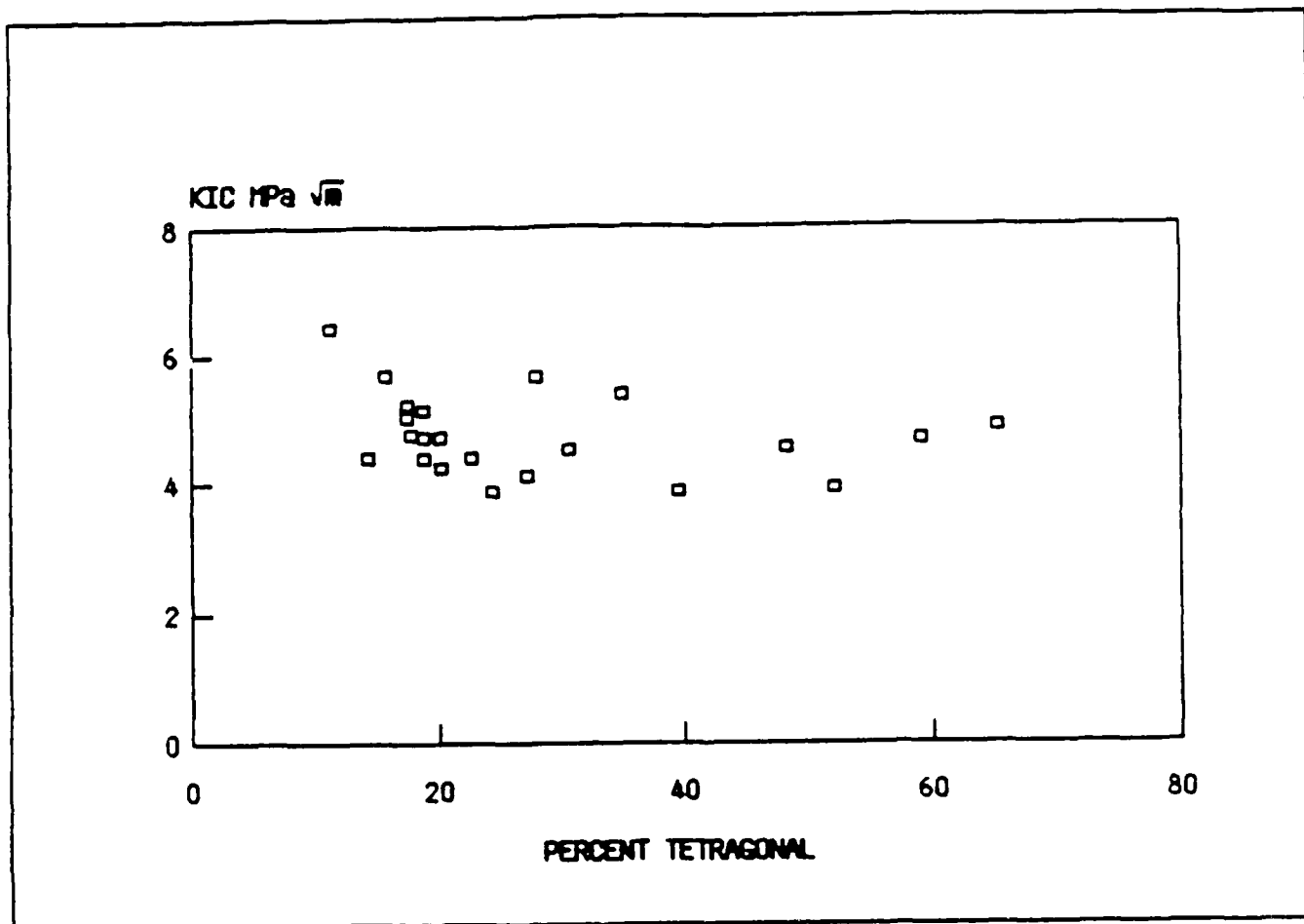


Figure 13. Fracture toughness versus percent tetragonal phase for 24 compositions of the Al<sub>2</sub>O<sub>3</sub> - Cr<sub>2</sub>O<sub>3</sub> / ZrO<sub>2</sub> - HfO<sub>2</sub> system.

TRANSFORMATION-TOUGHENED MULLITE

WITH

$\text{ZrO}_2/\text{HfO}_2$  SOLID SOLUTIONS

C.K. Yoon and T.Y. Tien  
Materials and Metallurgical Engineering  
The University of Michigan  
Ann Arbor, Michigan 48109

<p>Army Materials and Mechanics Research Center Watertown, Massachusetts 02172 TRANSFORMATION TOUGHENED CERAMICS - A POTENTIAL MATERIAL FOR LIGHT DIESEL ENGINE APPLICATIONS T. Y. Tien University of Michigan Ann Arbor, Michigan 48109</p> <p>Technical Report AMMRC TR 84-26, June 1984 48 pp -illus -tables, Contract DAAG 46-82-C-0080 Final Report - 1 October 1982 to 30 September 1983</p> <p>This report contains three parts: The thermal conductivity studies in the system <math>Al_2O_3-Cr_2O_3-ZrO_2-HfO_2</math> are presented in the first part. The mechanical behavior of these compositions will be presented in the second part. The mullite - <math>ZrO_2</math> system will be discussed in the third part. The results indicate that a composition containing 15 mole % of <math>Cr_2O_3</math> in the matrix phase has a thermal conductivity comparable to that of stabilized zirconia.</p>	<p>AD _____</p> <p>UNCLASSIFIED</p> <p>UNLIMITED DISTRIBUTION</p> <p>Key Words</p> <p>Thermal Conductivity Chromia Zirconia, Alumina Transformation Toughening</p>
<p>Army Materials and Mechanics Research Center Watertown, Massachusetts 02172 TRANSFORMATION TOUGHENED CERAMICS - A POTENTIAL MATERIAL FOR LIGHT DIESEL ENGINE APPLICATIONS T. Y. Tien University of Michigan Ann Arbor, Michigan 48109</p> <p>Technical Report AMMRC TR 84-26, June 1984 48 pp -illus -tables, Contract DAAG 46-82-C-0080 Final Report - 1 October 1982 to 30 September 1983</p> <p>This report contains three parts: The thermal conductivity studies in the system <math>Al_2O_3-Cr_2O_3-ZrO_2-HfO_2</math> are presented in the first part. The mechanical behavior of these compositions will be presented in the second part. The mullite - <math>ZrO_2</math> system will be discussed in the third part. The results indicate that a composition containing 15 mole % of <math>Cr_2O_3</math> in the matrix phase has a thermal conductivity comparable to that of stabilized zirconia.</p>	<p>AD _____</p> <p>UNCLASSIFIED</p> <p>UNLIMITED DISTRIBUTION</p> <p>Key Words</p> <p>Thermal Conductivity Chromia Zirconia, Alumina Transformation Toughening</p>
<p>Army Materials and Mechanics Research Center Watertown, Massachusetts 02172 TRANSFORMATION TOUGHENED CERAMICS - A POTENTIAL MATERIAL FOR LIGHT DIESEL ENGINE APPLICATIONS T. Y. Tien University of Michigan Ann Arbor, Michigan 48109</p> <p>Technical Report AMMRC TR 84-26, June 1984 48 pp -illus -tables, Contract DAAG 46-82-C-0080 Final Report - 1 October 1982 to 30 September 1983</p> <p>This report contains three parts: The thermal conductivity studies in the system <math>Al_2O_3-Cr_2O_3-ZrO_2-HfO_2</math> are presented in the first part. The mechanical behavior of these compositions will be presented in the second part. The mullite - <math>ZrO_2</math> system will be discussed in the third part. The results indicate that a composition containing 15 mole % of <math>Cr_2O_3</math> in the matrix phase has a thermal conductivity comparable to that of stabilized zirconia.</p>	<p>AD _____</p> <p>UNCLASSIFIED</p> <p>UNLIMITED DISTRIBUTION</p> <p>Key Words</p> <p>Thermal Conductivity Chromia Zirconia, Alumina Transformation Toughening</p>
<p>Army Materials and Mechanics Research Center Watertown, Massachusetts 02172 TRANSFORMATION TOUGHENED CERAMICS - A POTENTIAL MATERIAL FOR LIGHT DIESEL ENGINE APPLICATIONS T. Y. Tien University of Michigan Ann Arbor, Michigan 48109</p> <p>Technical Report AMMRC TR 84-26, June 1984 48 pp -illus -tables, Contract DAAG 46-82-C-0080 Final Report - 1 October 1982 to 30 September 1983</p> <p>This report contains three parts: The thermal conductivity studies in the system <math>Al_2O_3-Cr_2O_3-ZrO_2-HfO_2</math> are presented in the first part. The mechanical behavior of these compositions will be presented in the second part. The mullite - <math>ZrO_2</math> system will be discussed in the third part. The results indicate that a composition containing 15 mole % of <math>Cr_2O_3</math> in the matrix phase has a thermal conductivity comparable to that of stabilized zirconia.</p>	<p>AD _____</p> <p>UNCLASSIFIED</p> <p>UNLIMITED DISTRIBUTION</p> <p>Key Words</p> <p>Thermal Conductivity Chromia Zirconia, Alumina Transformation Toughening</p>

From	To	No. of Copies
1 Norton Company, Turbine Research Department, Westland Avenue, Dearborn, MI 48121	Norton Company, Worcester, MA 01606	1
ATTN: Mr. A. E. McLean	ATTN: Dr. W. Ault	1
Mr. A. Ezzis	Dr. M. L. Fort	
Mr. D. A. Mangels	Pennsylvania State University, Materials Research Laboratory, Materials Science Department, University Park, PA 16802	
Dr. R. Govila	ATTN: Prof. R. E. Tressler	1
Mr. R. Baker	Prof. V. S. Stubbins	1
General Electric Company, Research and Development Center, Schenectady, NY 12345	RIAS, Division of the Martin Company, Baltimore, MD 21202	
ATTN: Dr. R. L. Charles	ATTN: Dr. A. R. C. Westwood	1
Dr. J. D. Greskovich		
Dr. D. Prochazka	Stanford Research International, 333 Ravenswood Avenue, Menlo Park, CA 94025	
Georgia Institute of Technology, EES, Atlanta, GA 30332	ATTN: Dr. P. Jorgensen	1
ATTN: Mr. J. K. Walton	Dr. D. Rowcliffe	1
MIT Laboratories, Waltham Research Center, 40 Sylvan Road, Waltham, MA 02154	State University of New York at Stony Brook, Department of Materials Science, Long Island, NY 11790	
ATTN: Dr. J. Gracknash	ATTN: Prof. Franklin F. Y. Wang	1
Dr. W. M. Rhodes		
MIT Research Institute, 11 West 35th Street, Chicago, IL 60616	United Technologies Research Center, East Hartford, CT 06103	
ATTN: Mr. J. Spritz, Director, Ceramics Research	ATTN: Dr. J. Brennan	1
	Dr. F. Galasso	1
Institut für Werkstoff-Forschung, DLR, Bunsenstrasse, D-1000 Berlin, Germany	University of California, Lawrence Livermore Laboratory, P. O. Box 808, Livermore, CA 94550	
ATTN: Dr. A. Kien	ATTN: Dr. C. E. Sline	1
International Harvester, 1000 Olive Street, 1200 Pacific Highway, Oak Brook, Illinois, USA 60151	University of Florida, Department of Materials Science and Engineering, Gainesville, FL 32601	
ATTN: Dr. A. Metcalfe	ATTN: Dr. L. Hench	1
Flowtek Service Industries, Inc., P.O. Box 146, Reading, PA 19605	University of Newcastle Upon Tyne, Department of Metallurgy and Engineering Materials, Newcastle Upon Tyne, NE1 7RU, England	
ATTN: Mr. W. J. Longnecker	ATTN: Prof. K. H. Jack	1
Martin Marietta Laboratories, 1450 South Rolling Road, Baltimore, MD 21127	University of Washington, Ceramic Engineering Division, FB-10, Seattle, WA 98195	
ATTN: Dr. J. Venables	ATTN: Prof. James I. Mueller	1
	Prof. R. Bradt	1
Massachusetts Institute of Technology, Department of Metallurgy and Materials Science, Cambridge, MA 02139	Westinghouse Electric Corporation, Research Laboratories, Pittsburgh, PA 15235	
ATTN: Prof. R. L. Noble	ATTN: Dr. R. J. Bratton	1
Prof. H. N. Bowen		
Prof. W. D. Kingery		
Midwest Research Institute, 435 Jackson Boulevard, Springfield, MO 64110	Director, Army Materials and Mechanics Research Center, Watertown, MA 02172	
ATTN: Mr. Gordon W. Gross, Head, Physics Station	ATTN: DRXMR-PL	1
	DRXMR-PAT	1
	DRXMR-K	1
	DRXMR-MC, Schriber	10

No.	of Copies
1	Commander, U.S. Air Force Wright Aeronautical Laboratories, Wright-Patterson Air Force Base, OH 45433 ATTN: AFVAL/MLLM, Dr. N. Tallian AFVAL/MLLM, Dr. H. Graham AFVAL/MLLM, Dr. R. Ruh AFVAL/MLLM, Dr. A. Katz AFVAL/MLLM, Mr. K. S. Mazdiyassni Aero Propulsion Labs, Mr. R. Marsh
1	National Aeronautics and Space Administration, Washington, DC 20546 ATTN: Mr. C. Bush AFSS-AD, Office of Scientific and Technical Information
1	National Aeronautics and Space Administration, Lewis Research Center, 11000 Brookpark Road, Cleveland, OH 44135 ATTN: J. Accurio, USAMRDL Dr. M. B. Probst, MS 49-1 Mr. G. Dutta
1	National Aeronautics and Space Administration, Langley Research Center, Hampton, VA 23665 ATTN: Mr. W. Buckley, Mail Stop 357
1	Department of Energy, Division of Transportation, 10 Massachusetts Avenue, N.W., Washington, DC 20545 ATTN: Mr. Robert Schultz (TEC)
1	Department of Transportation, 400 Seventh Street, S.W., Washington, DC 20590 ATTN: Mr. M. Lauriente
1	National Bureau of Standards, Washington, DC 20234 ATTN: Dr. G. Wiederhorn
1	National Research Council, National Materials Advisory Board, 1101 Constitution Avenue, Washington, DC 20418 ATTN: D. Groves R. M. Spriggs
1	Admiralty Materials Technology Establishment, Poole, Dorset BH16 9DU, UK ATTN: Dr. D. Godfray Dr. M. Lindlev
1	AirResearch Manufacturing Company, AirResearch Casting Company, 2525 West 190th Street, Torrance, CA 90505 ATTN: Mr. K. Styhr
1	AirResearch Manufacturing Company, Materials Engineering Dept., 111 South 4th Street, P.O. Box 5217, Phoenix, AZ 85010 ATTN: Mr. D. W. Richardson, MS 98-393/503-44
1	AVCO Corporation, Applied Technology Division, Lowell Industrial Park, Lowell, MA 01850 ATTN: Dr. I. Vasilos
1	Carborundum Company, Research and Development Division, P.O. Box 1024, Niagara Falls, NY 14304 ATTN: Dr. D. W. Coppola
1	General Western Research Laboratory, Department of Metallurgy, Cleveland, OH 44116 ATTN: Mr. A. M. Brown
1	Cummins Engine Company, Columbus, IN 47201 ATTN: Mr. R. Kamo Mr. J. Patton
1	Electric Power Research Institute, P.O. Box 1441, 311 Middlesex Avenue, Palo Alto, CA 94304 ATTN: Mr. R. John
1	European Space Agency, 111 Mary Queen's Road, London, SW1E 5BT, England ATTN: Mr. J. Luth Mr. J. Palmer-Sweeney
1	General Electric Aircraft Engines Division, General Electric Corp., P.O. Box 100, Hartford, CT 06155 ATTN: Mr. J. E. ...

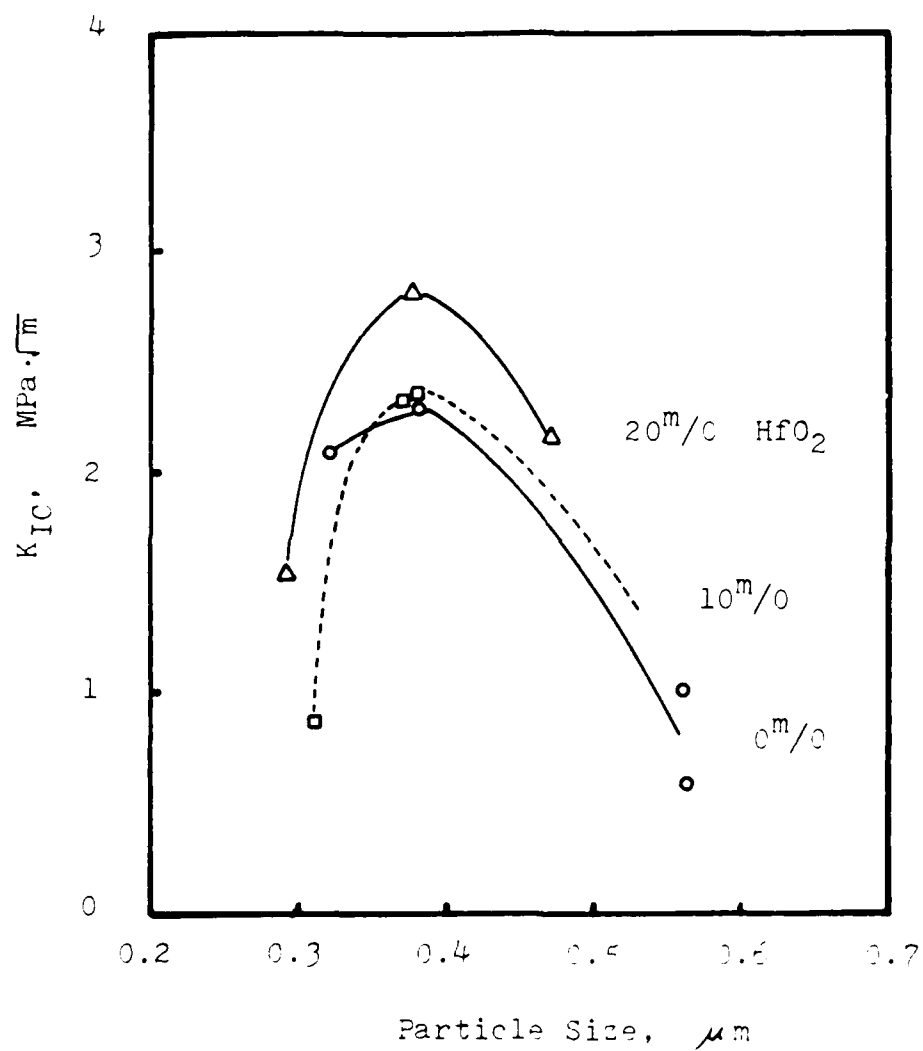


Fig. 7. Variations of  $K_{IC}$  values with particle sizes at different  $\text{HfO}_2$  contents. (sintered at  $1650^\circ\text{C}$ )

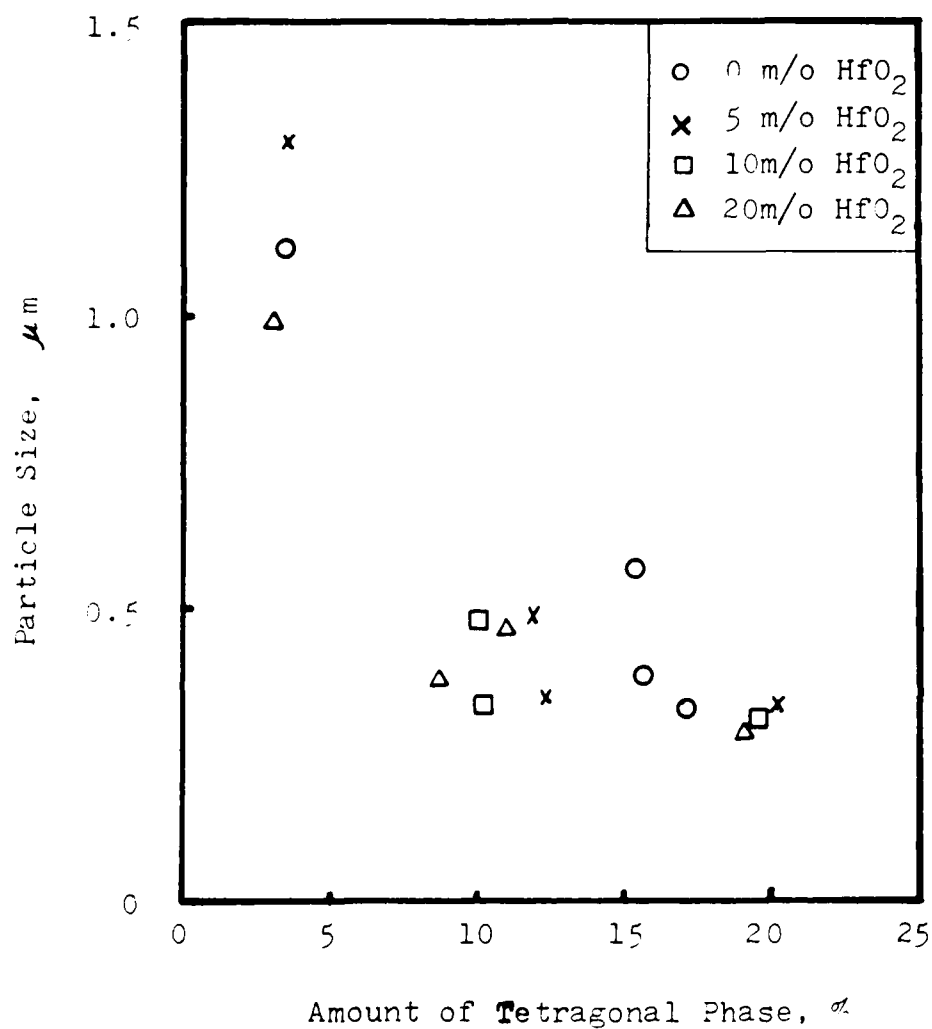


Fig. 6. Variations of the amount of tetragonal phase with particle sizes (sintered at  $1650^{\circ}\text{C}$ ).



0%  $\text{HfO}_2 \rightarrow$  (a) 0.5 hr.



20%  $\text{HfO}_2 \rightarrow$  (d) 0.5 hr.



(b) 2 hr.



(e) 2 hr.



(c) 5 hr.



(f) 5 hr.

Fig. 6. SEM microstructures of mullite with  $\text{ZrO}_2/\text{HfO}_2$  dispersions at different  $\text{HfO}_2$  content and times at  $1650^\circ\text{C}$ . Thermally etched.



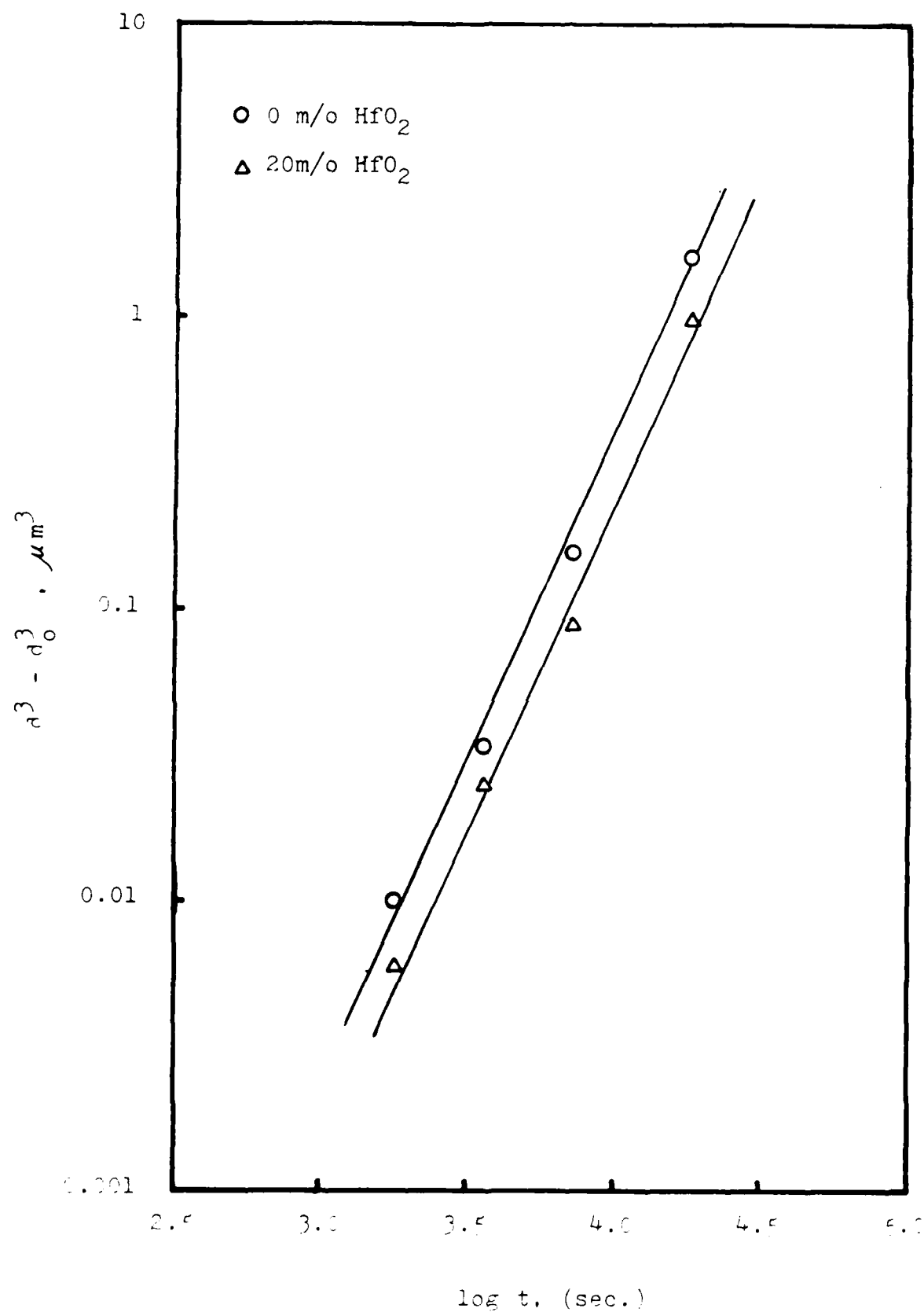


Fig. 4. Log-log plot of isothermal particle growth with sintering time at  $1650^\circ\text{C}$ .

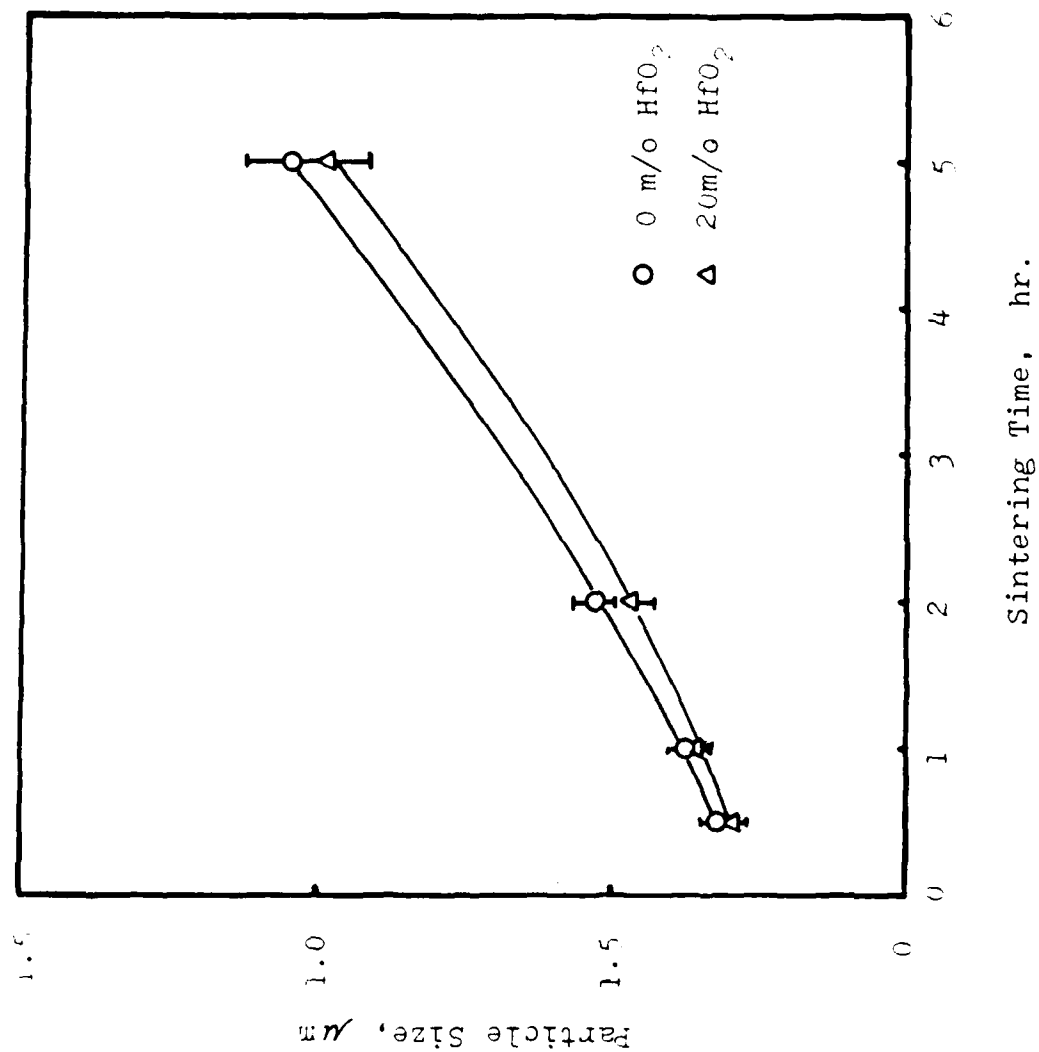


Fig. 3. Variations of particle size with changing sintering time at  $1650^\circ\text{C}$ .

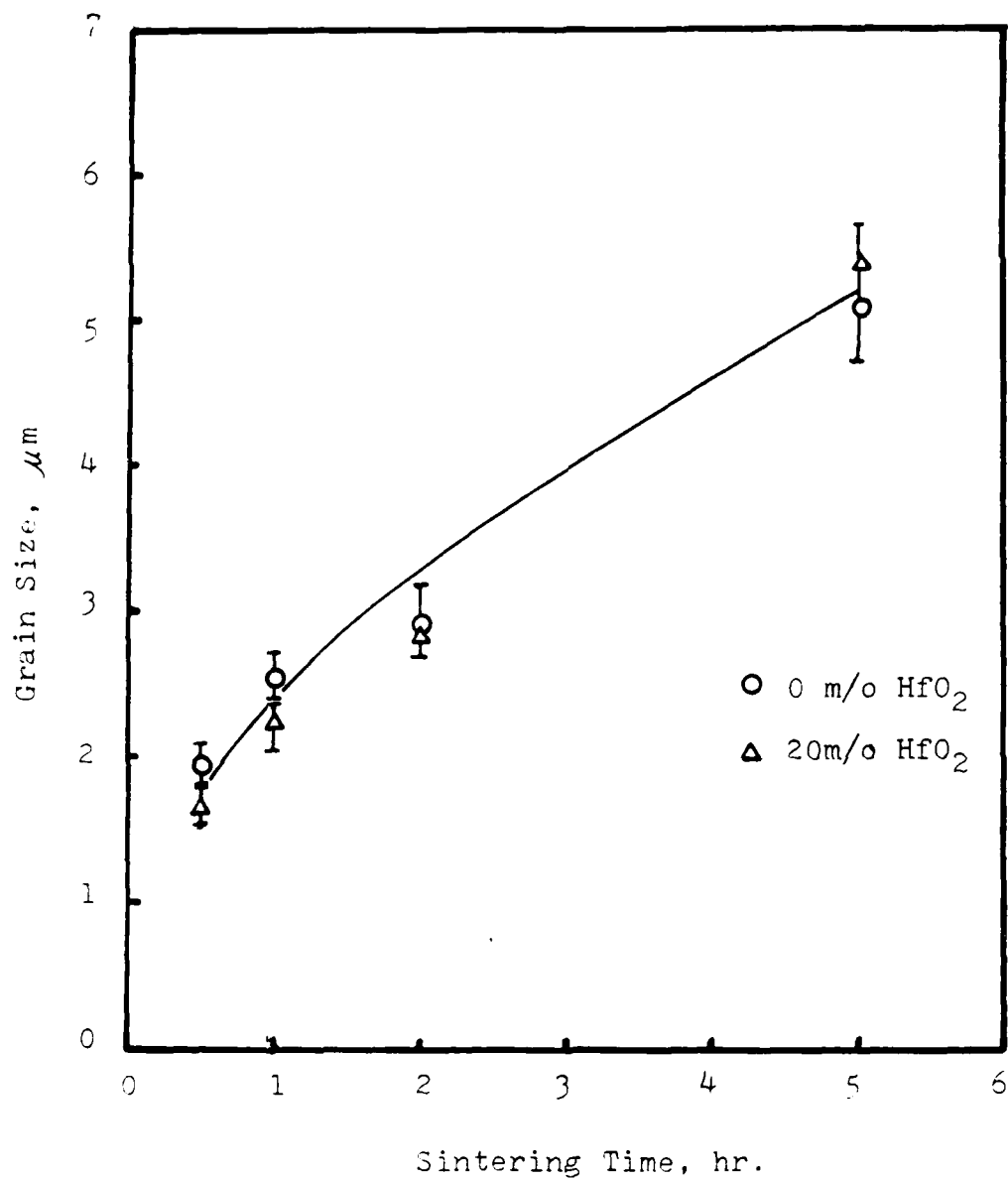


Fig. 2. Grain growth behavior with changing the sintering time at 165. °C.

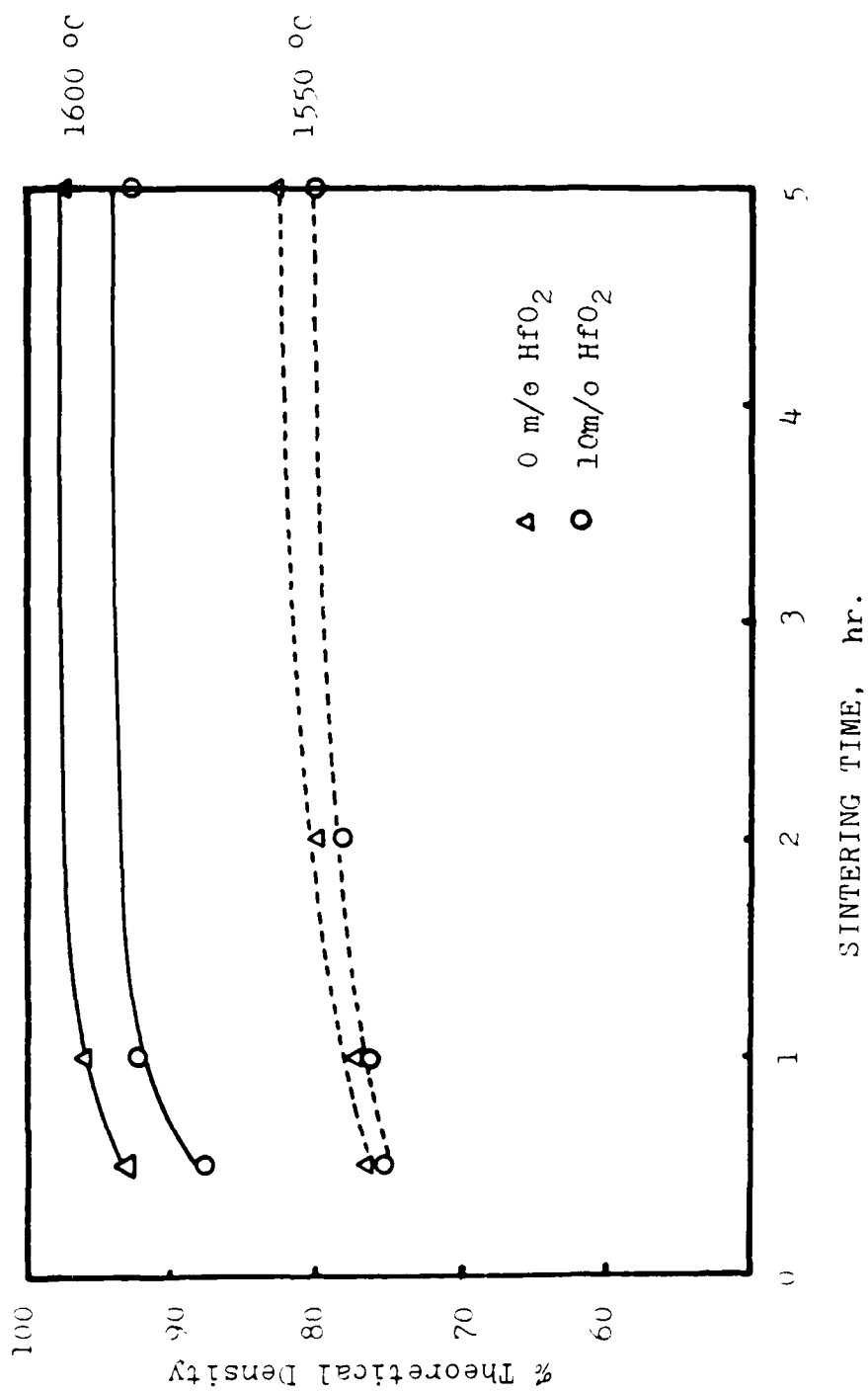


Fig. 1. Variation of %theoretical density with sintering time at different temperatures.

## REFERENCES

1. Lange, F.F., Transformation Toughening: Part 1, J. Mat. Sci., 17, (1982), 225-234.
2. Claussen, N., Sigulinski, F., and Ruhle, M., Phase Transformation of Solid Solutions of  $ZrO_2$  and  $HfO_2$  in a  $Al_2O_3$  Matrix, Advances in Ceramics, Vol. 3, The American Ceramic Society, Inc., 1981, 164-167.
3. Ruf, H., and Evans, A.G., Toughening by Monoclinic  $ZrO_2$ , J. Am. Ceram. Soc., 66, (1983), 328-332.
4. McMeeking, R.M., and Evans, A.G., Mechanics of Transformation Toughening in Brittle Materials, J. Am. Ceram. Soc., 65, (1982), 242-246.
5. Claussen, N., Steeb, J., and Pabst, R.F., Effect of Induced Micro-cracking on the Fracture Toughness of Ceramics, J. Am. Ceram. Soc., 56, (1977), 559-562.
6. Claussen, N., and Ruhle, M., Design of Transformation-Toughened Ceramics, Advances in Ceramics, Vol. 3, The American Ceramic Society, Inc., 1981, 137-163.

indicate that the grain growth of the dispersed phase is a diffusional process.

The microstructures shown in Figure 5 show that the presence of  $\text{HfO}_2$  does not appear to affect the microstructural development. These specimens were sintered at  $1650^\circ\text{C}$  for .5, 2, and 5 hours. Mullite grains in the sintered specimens appeared to be elongated and the dispersed phase is located at intergranular sites. The particle size as a function of percent tetragonal phase is shown in Figure 6. The amount of tetragonal phase increases with decreasing particle size.

Figure 7 shows the variation of  $K_{IC}$  with particle size for several hafnia contents. The fracture toughness increased with increasing hafnia content for a constant particle size. All three curves in Figure 7 showed a maximum indicating the critical particle size of the dispersed phase. Therefore, the control of the particle size in a given matrix seems to be an important factor for fracture toughness improvement.

#### CONCLUSIONS

1. Hafnia additions in zirconia inhibited the growth of the dispersed phase.
2. The fracture toughness was increased by the addition of  $\text{HfO}_2$ .
3. The critical particle size of  $\text{ZrO}_2/\text{HfO}_2$  dispersions in mullite was approximately 0.4 microns.

Bulk densities were measured using Archimedes' principle using water as the media. Phase identification was done by x-ray diffraction and by microstructural examination of the polished and thermally etched surface. Fracture toughness values for some of the specimens were measured by the microindentation method. Five indentations were made at each of five different load levels. The amount of tetragonal phase for each specimen was obtained by measuring the (111) tetragonal peak and the (11 $\bar{1}$ ) monoclinic peak.

## RESULTS AND DISCUSSION

Figure 1 shows the bulk densities of sintered specimens. The specimens sintered at 1500°C did not densify (75-82% theoretical density). Specimens sintered at temperatures above 1600°C for a period longer than one hour reached 95% theoretical density. As shown in Figure 1, the presence of HfO<sub>2</sub> in the dispersed phase seems to retard the densification of the composites.

All specimens sintered at 1550°C and 1600°C contained ZrSiO<sub>4</sub>. The zircon phase disappeared at 1650°C. Therefore, all specimens for further studies were sintered at 1650°C.

Grain growth data at 1650°C are shown in Figure 2. The grain growth rate was affected by the presence of hafnia in the dispersed phase. Changes in the dispersed phase particle size for specimens sintered at 1650°C are given in Figure 3. The particle size decreased slightly with HfO<sub>2</sub> additions. Figure 4 is a plot of  $d^3 - d_0^3$  versus sintering time at 1650°C for specimens containing 0 and 20 m/o HfO<sub>2</sub>. The straight lines

## ABSTRACT

Mullite with dispersions of solid solutions of  $\text{ZrO}_2/\text{HfO}_2$  was studied. With the addition of hafnia to zirconia, the fracture toughness was increased and the growth rate of the dispersed phase was slightly suppressed. A "critical particle size" was found to be approximately 0.4  $\mu\text{m}$ .

## MATERIALS AND EXPERIMENTAL PROCEDURE

Four compositions in the mullite-zirconia-hafnia system were studied. The volume fraction of dispersed phase was kept constant at 15 v/o. The hafnia content in  $\text{ZrO}_2/\text{HfO}_2$  solid solution was varied from 0-20 m/o (0, 5, 10, and 20 m/o).

Aqueous solutions of aluminum nitrate, zirconium oxychloride, hafnium oxychloride, and tetraethoxysilane were used as starting materials. Appropriate amounts of solution were mixed and ethanol was added to the mixtures to prevent separation of the ethoxysilane from the aqueous solution. Mixed solutions were stirred for 30 min. and  $\text{NH}_4\text{OH}$  was slowly added to the mixtures. When the pH value reached 5.5 a stiff gel formed. The gel was filtered, dried at  $100^\circ\text{C}$ , and calcined at  $450^\circ\text{C}$  for one hour. The calcined powders were amorphous to x-rays. The powders were ground in an agate jar mill with agate balls for 7 hours. The ground powders were isostatically pressed at 135 MPa and sintered at 1550, 1600, and  $1650^\circ\text{C}$  for 30 min., one, two, and five hours.



**END**

**FILMED**

**4-85**

**DTIC**